Chemical vapour deposition diamond studied by optical and electron spin resonance techniques

2002 J. Phys.: Condens. Matter 14 R467

(http://iopscience.iop.org/0953-8984/14/17/202)

INSTITUTE OF PHYSICS PUBLISHING JOURNAL OF PHYSICS: CONDENSED MATTER

J. Phys.: Condens. Matter **14** (2002) R467–R499 PII: S0953-8984(02)19765-7

TOPICAL REVIEW

Chemical vapour deposition diamond studied by optical and electron spin resonance techniques

K Iakoubovskii and A Stesmans

Laboratorium voor Halfgeleiderfysica, Katholieke Universiteit Leuven, Celestijnenlaan 200 D, 3001 Leuven, Belgium

E-mail: kostya.iak@fys.kuleuven.ac.be

Received 1 March 2002
Published 18 April 2002
Online at stacks.iop.org/JPhysCM/14/R467

Abstract

This work discusses the current situation in the study of bulk defects in diamond, grown by chemical vapour deposition (CVD), using optical absorption, luminescence, and electron spin resonance techniques. CVD diamond appears distinct from other types of diamond in that it exhibits significant concentrations of bulk defects involving hydrogen, silicon, and possibly tungsten impurities. Importantly, as regards doping, p-type conductivity up to the degeneracy level can be achieved by boron incorporation, while n-type conductivity can be realized by phosphorus doping. A generally observed trend is cross fertilization between the studies of various types of diamond: the knowledge of the properties of intrinsic and irradiation-induced defects, obtained from extensive studies of natural and high-pressure synthetic diamond crystals, helps in understanding the presence of certain radiation-damage-related centres in as-grown CVD films. In return, some achievements from the study of defect centres in CVD diamond may provide useful information for modelling of defects in crystalline diamond and other semiconducting materials.

List of abbreviations and symbols

α	absorption coefficient
a-C	amorphous carbon
CL	cathodoluminescence
CVD	chemical vapour deposition
DA	donor–acceptor (pair)
E_C	conductance band edge energy
E_V	valence band edge energy
e–h	electron–hole
ERD	elastic recoil detection
ESR	electron spin resonance
hf	hyperfine
HPHT	high-pressure high-temperature
IR	infrared
LESR	light-induced electron spin resonance
LVM	local vibrational (or vibronic) mode
NAA	nuclear activation analysis
NMR	nuclear magnetic resonance
ODMR	optically detected magnetic resonance
PC	photoconductivity
PL	photoluminescence
PLE	photoluminescence excitation
ppb	(atomic) parts per billion (10^{-9})
ppm	(atomic) parts per million (10^{-6})
SIMS	secondary-ion mass spectroscopy
SO	spin–orbit
T_{an}	the minimal temperature required to anneal out a defect
VXV	divacancy with an impurity X in the centre
V–X_S–V	two vacancies separated by a substitutional impurity X
ZPL	zero-phonon line

1. Introduction

Diamond grown by chemical vapour deposition (CVD) is a technologically important and physically interesting material. Currently, comprehensive reviews exist on the growth and macroscopical (electronic, mechanical, optical, thermal, electrochemical, etc) properties of CVD diamond (see, e.g., Lettington and Steeds (1993), Spear and Dismukes (1994), Pan and Kania (1995), Liu and Dandy (1996), Prelas *et al* (1997), Werner and Locher (1998), Dischler (1998), Piekarczyk (1999), Lee *et al* (1999), Wilson and Jubber (1999), Asmussen and Reinhard (2001), Nazaré and Neves (2001)), while data on defect centres in CVD diamond are largely lacking. In an attempt to fill this gap, the current status of the study and understanding of bulk defects in CVD diamond is reviewed in this article. After a short introduction to the common classification scheme for diamond, some measurement techniques, pertinent to the investigation of defects in diamond, are briefly discussed. Although the work will focus on those defects characterized by optical and electron spin resonance (ESR) techniques, two other methods, i.e., ion channelling and secondary-ion mass spectroscopy (SIMS), are briefly

discussed also, as some results obtained by these methods bear relevance to the field. Before starting the description of defect centres in CVD diamond, a brief analysis of basic defects in the much more intensively studied natural and high-pressure high-temperature (HPHT) synthetic diamonds is given. Also, some peculiarities of a common CVD growth process are addressed in order to provide a clue to the understanding of defect formation in CVD diamond.

The overview is necessarily subject to restrictions: centres involving more than one nitrogen atom, except for the basic A, B, H2, and H3 complexes (vide infra), are not considered because of their apparently minor importance for this material. Also, centres produced in CVD diamond by post-growth irradiation with high-energy (>100 keV) particles (hereafter referred to as irradiation), which have been already identified in natural and HPHT diamond, will not be addressed. It will then appear that most of the defects thus far detected in CVD diamond involve an impurity, according to which they are classified.

2. Classification of diamonds

According to the production method, nowadays one commonly distinguishes natural, HPHT, and CVD diamonds. *Natural* diamonds are traditionally subdivided into four types, i.e., Ia, Ib, IIa, and IIb, according to the dominant type of defect present. More than 95% of all natural diamonds belong to type Ia, where the dominant defect encountered is aggregated nitrogen. This type is further divided into two subtypes: in the IaA subtype, nitrogen is present in the form of nearest-neighbour substitutional pairs ($[N_S–N_S]^0$ or the A centre), while it occurs as a complex of four substitutional nitrogen atoms bordering a lattice vacancy ($[4N_S–V]^0$ or the B centre) in the IaB subtype. In the rare natural type Ib, the dominant defect is the single-substitutional nitrogen donor centre, variably labelled as the N_S, P1, or C centre.

Type IIa refers to pure stones, in which the nitrogen impurity level is below the IR absorption detectivity ($\sim$1 ppm). In type IIb diamond, boron is the dominant impurity. This type shows semiconductor properties caused by the presence of uncompensated single-substitutional boron acceptors (B_S^0). In contrast, type Ia, Ib, and IIa crystals exhibit no measurable conductivity at ambient conditions.

Many of the origins of the various types were inferred from laboratory experiments on growth and annealing of HPHT diamonds: at the HPHT conditions of diamond growth, the nitrogen impurity is dissolved as single atoms in the seed material utilized, and the synthesis typically occurs at relatively low temperatures (1200–1400 °C). Consequently, most as-grown HPHT diamonds are of the type Ib. Type IIb crystals can be produced if boron is intentionally added into the growth chamber and the nitrogen content is reduced, e.g., by using Ti, Zr, Al, or other getters. High-temperature annealing of Ib diamond results in the aggregation of single-substitutional nitrogen to A (at $T > 1500$ °C) and then to B ($T > 2400$ °C) complexes (Evans and Qi 1982). Most natural diamonds are older than 1 Gyr and, consequently, nitrogen in these is largely aggregated.

3. Some techniques of defect characterization in diamond

3.1. Optical absorption and luminescence

The above classification of diamond relies on the IR absorption measurements. The diamond lattice has an inversion centre that forbids one-phonon absorption. Therefore, experimentally observed absorption in the one-phonon region of the spectrum is attributed to the reduction of local lattice symmetry by the presence of defects. The one-phonon absorption coefficient can be converted into the impurity concentration using calibrations (Davies 1999), obtained with

combustion analysis, nuclear activation analysis (NAA), or other nuclear methods, such as SIMS and elastic recoil detection (ERD). Information on vibrational frequencies of a defect, obtained from IR spectra, can be much enriched with results of UV–visible absorption and photoluminescence (PL) and cathodoluminescence (CL) techniques which detect electron–phonon transitions. With the help of uniaxial-stress (Davies 1979, Davies and Hammer 1976, Davies and Nazaré 1980) or polarization-resolved measurements (Brown and Rand 1995) the symmetry of a centre can be deduced. By analysing the shift of the optical peaks with isotopic substitutions, one can obtain information on the constituents of the corresponding defect centre (Davies 1999).

There is a tremendous gain in sensitivity when detecting electronic, rather than vibrational transitions. While IR spectroscopy has a typical sensitivity of $\sim$1 ppm, a detection level of 0.1 ppm and less can be reached in visible–UV absorption, and a single defect centre can be characterized by PL (Gruber *et al* 1997). Apparently, a single defect centre in diamond (in particular, the $[N_S–V]^-$ centre) is an attractive object of study. This interest partially originates from the fact that most single-molecule optical centres are bleached after emission of $\sim 10^6$–10^8 photons at room temperature (Soper *et al* 1993), while PL from a single $[N_S–V]^-$ centre is stable over time (Gruber *et al* 1997).

More than 500 electronic and more than 150 vibrational optical centres have been documented for diamond, about half of them being impurity related (Zaitsev 2000, 2001). An optical centre in diamond is traditionally characterized by the position of its zero-phonon line (ZPL) at 77 K. However, there are a large number of known ZPLs, especially in the visible range. So, in order to identify an optical centre in diamond, one has to compare not only the ZPL position, but also the shape of the whole relevant vibronic spectrum, its temperature behaviour, production history, relaxation time, etc. The most comprehensive catalogues of optical lines and spectra in all types of diamond were compiled by Zaitsev (1998, 2001). A table of Ni-related optical absorption lines (*henceforth we shall drop the adjective 'optical' throughout the text*) can be found in a paper by Yelisseyev and Nadolinny (1995). For more in-depth description of optical centres in diamond we suggest the reviews by Davies (1999), Collins (1992, 1993, 1999) and Walker (1979) on intrinsic and nitrogen-related optical centres; by Gippius *et al* (1983), Gippius (1993) and Zaitsev (1993) on luminescence centres produced by ion implantation; by Collins (2000) and Zaitsev (2000) on metal-related optical centres; by Lawson *et al* (1996) on Co-related optical lines. For analysis of vibronic coupling, Jahn–Teller and uniaxial-stress-induced effects one may refer to works of Davies (1974, 1979, 1981).

The production mechanism of ZPLs in CL or in PL, excited by above-band-gap light, is not clear. Such excitation produces electron–hole (e–h) pairs. It was proposed (Khong and Collins 1993) that capture of an e–h pair leads to the transition of a defect centre X from the ground state X_0 to an excited X^* state according to the reaction $X_0 + (e–h) \rightarrow X^* \rightarrow X_0 + h\nu$, and noted that some optical centres in diamond can be observed in PL, but not in CL. As a possible explanation suggested for the latter phenomenon was that negatively charged centres (or, in general, centres with a weakly bound electron) become not excited, but ionized upon capturing an e–h pair (Iakoubovskii *et al* 2000a).

The integrated intensity of the luminescence or absorption system is proportional to the concentration of the corresponding optical centre. Luminescence intensity is also affected by many other factors, especially by the experiment design and by the lifetime of the excited states, which can be strongly sample dependent. Therefore, the concentration of an optical centre is usually determined not from PL, but from absorption spectra: the integral over the corresponding ZPL, measured at 77 K, is multiplied by the inferred calibration coefficient (Davies 1999). This procedure relies upon the constancy of the integrated intensity ratio of the ZPL to the total vibronic system. Yet, it has two major drawbacks:

(1) The above-mentioned ratio and, therefore, the calibration coefficient are temperature dependent. This makes it mandatory to stick to the temperature at which the calibration was performed (77 K).
(2) Furthermore, that ratio may depend on strain in the sample. A typical example is the GR1 vibronic band: the intensity of its ZPL at 1.673 eV depends on irradiation dose and defect content in diamond (e.g., Clark *et al* (1956)).

In some cases, in order to estimate the concentration of an optical centre from optical absorption, it may be more reliable to use the integral not over a ZPL, but over the whole vibronic band. The latter integral is independent of strain and temperature, as far as electron–phonon coupling is concerned (Davies 1981). Meanwhile, the correlation coefficients can be recalculated for the whole vibronic band using data obtained on low-stress samples (see Davies *et al* (1992)).

3.2. Electron spin resonance

The above-mentioned optical methods can yield the symmetry and impurity content of a defect centre, its energy levels, and the vibronic modes. However, conclusive information on the types of atom involved and their arrangement in a centre is generally deduced from ESR measurements via analysis of the hyperfine (hf) interaction structure. More than a hundred ESR spectra for diamond have been documented. The most comprehensive ESR tables were compiled by Ammerlaan (1989) and Newton (1994). For more in-depth analysis of basic ESR spectra in diamond we refer the reader to a series of papers by the Oxford diamond group (Baker and Newton 1994, 1995, Hunt *et al* 2000a, b Twitchen *et al* 1996, 1999a, b), by Isoya *et al* (1990a, 1990b, 1992), and by van Wyk *et al* (1995). Recent results on Ni- and Co-related ESR centres can be found in papers by Nadolinny *et al* (1997, 1999), Neves *et al* (2000), and Twitchen *et al* (2000).

All ESR spectra mentioned in this paper have been interpreted using the spin Hamiltonian

$$H = \mu_e \boldsymbol{S} \cdot \mathbf{g} \cdot \boldsymbol{B} + \sum (\boldsymbol{S} \cdot \mathbf{A}_i \cdot \boldsymbol{I}_i + g_{\mathrm{N},i} \mu_{\mathrm{N}} \boldsymbol{I}_i \cdot \boldsymbol{B}) + \boldsymbol{S} \cdot \mathbf{D} \cdot \boldsymbol{S}. \quad (1)$$

Here, μ_ε and μ_{N} are the electron and nuclear magnetons, respectively, and g_{N} is the nuclear g-factor. The first term in (1) describes the electron Zeeman interaction of an electronic system of spin $\boldsymbol{S}$ with the applied magnetic field $\boldsymbol{B}$ via the electronic $\mathbf{g}$-tensor. The second term accounts for the hf interaction of the electronic spin system with nuclei of spin $\boldsymbol{I}_i$ via the hf matrix $\mathbf{A}_i$. The third term is due to interaction of the nuclear spin with the magnetic field. Because of the small value of the product $g_{\mathrm{N}}\mu_{\mathrm{N}}$ for most nuclei, it gives only higher-order corrections to the electronic terms. However, for such isotopes as ^{1}H, ^{3}H, ^{3}He, ^{19}F, the nuclear Zeeman term can become comparable with the second one. In the latter case, it significantly affects the hf interaction structure, in particular by increasing the strength of normally forbidden spin-flip transitions ($\Delta m = 1$, where m is the quantum number corresponding to spin $\boldsymbol{I}$). The fourth term in (1) characterizes spin–spin interaction via a traceless matrix $\mathbf{D}$. This term vanishes in the case of tetrahedral symmetry or for $S = 1/2$. It can be rewritten as $\boldsymbol{S} \cdot \mathbf{D} \cdot \boldsymbol{S} = D_{ZZ}S_Z^2 + D_{YY}S_Y^2 + D_{XX}S_X^2 = D[S_Z^2 - S(S+1)/3] + E(S_X^2 - S_Y^2)$, where $D = 3D_{ZZ}/2$ and $E = |D_{XX} - D_{YY}|/2$, with the z-coordinate chosen along the defect axis. The sensitivity of a state-of-the-art ESR spectrometer, with intense signal averaging facility, is currently at the level of $\sim 10^{10}$ spins mT^{-1} for signals of less saturability. For example, for a linewidth of 0.17 mT and a diamond volume of 0.1 cm^3, this gives a figure of 10^{-7} ppm. This sensitivity can be tremendously increased in optically detected magnetic resonance (ODMR), where detection of a single defect centre has been demonstrated (Gruber *et al* 1997). Another advantage of ODMR is that it links optical and ESR spectra. Unfortunately, it has only been possible to study a few defect centres in diamond by this technique so far, namely the nitrogen

vacancy (Gruber *et al* 1997, van Oort *et al* 1990) and some Ni-related centres (Pavlik *et al* 1998, Nazaré *et al* 1995, Pereira *et al* 1994, Wesra *et al* 1992).

Most successfully, ESR is applied to single crystals, where basic information is obtained from mapping the angular dependence of spectral parameters, such as the g-factor, on the direction of $\boldsymbol{B}$. However, in CVD diamond samples with randomly oriented grains, the observed ESR signals exhibit the specific 'powder pattern' shape (see, e.g., figures 3 and 4, which will be discussed further), representing an average over all magnetic angles. As one consequence, this grain 'smearing' results in a loss of direct access to the relationship of specific principal-axis directions of the spin Hamiltonian to the crystallographic directions. The angle-dependent data, however, are now contained in the particular powder pattern shape, from where the spin Hamiltonian parameters are inferred by fitting to the shape function rigorously calculated on the basis of the proper resonance condition.

3.3. Ion channelling

Ion channelling (or just channelling) relies on detection of high-energy particles emitted during the decay of radioactive isotopes introduced into the crystal studied. From the analysis of the measured angular variation of the emission intensity, the lattice site of radioactive impurity can be deduced. Unfortunately, fast decay of many isotopes often leaves no time for post-implantation annealing in ion channeling experiments. The method has been successfully applied to Li, B, P, Ge, As, In, Cd, and Hf (Doyle *et al* 2000) ions implanted into natural and HPHT diamonds. Amazingly, high substitutional fractions, namely 70, 55, 54, and 34%, were observed for large (relative to carbon) As, P, Ge, and In atoms, respectively (Ronning and Hofsass 1999, Braunstein and Kalish 1981, Gorbatkin *et al* 1991, Bharuth-Ram *et al* 1995, 2001, Correia *et al* 1997), but only ∼12% of implanted boron was found in substitutional sites (Ittermann *et al* 1997). It was deduced that about 40% of all implanted Li atoms fill tetrahedral interstitial sites, about 17% go into substitutional sites, and the rest occupy random positions (Restle *et al* 1995, Ronning and Hofsass 1999). No variation in this distribution was observed for implantation temperatures in the range 100–900 K, suggesting that no detectable diffusion of *implanted* Li in diamond occurs, at least in that temperature range.

Applied to CVD diamond, ion channelling reveals that 90–100% of boron and about 80% of nitrogen atoms incorporate into the substitutional sites *during the growth* of homoepitaxial CVD films (Samlenski *et al* 1996).

3.4. Secondary-ion mass spectroscopy; diffusion in diamond

SIMS is one of the most popular techniques for studying diffusion in diamond, but it has a serious drawback (Shaanan and Kalish 2000, Fizgeer *et al* 2001): if after some technological treatment, impurity atoms still remain on the sample surface or in the subsurface region, then they can be recoiled into the sample by the probing ions (typically Cs^+ or O^+), creating an erroneous 'diffusion profile'. Consequently, many results on diffusion in diamond obtained by SIMS, especially on light elements, such as H, B, Li, O, may need to be treated with caution. For example, this notion provided an explanation for the unusual results on traditional ($T \sim 800\,^\circ$C, time $t \sim 2$ h) and electric-field-enhanced (E-enhanced) ($T \sim 800\,^\circ$C, $t \sim 2$ h, $E < 10^4$ V cm^{-1}) diffusion in single-crystal diamond obtained by Popovici *et al* (1995a,b, 1997): similar SIMS profiles, decaying from the surface to the bulk, have been measured for H, B, N, O, and F atoms—the observation being more characteristic for the recoil than for the diffusion mechanism. However, where the surface was carefully cleaned before SIMS measurement or introducing the dopant atoms by ion implantation at 77, 300, or 600 K, no detectable diffusion of Li and B was observed after annealing in the range 700–1400 °C, with

Table 1. Some parameters of basic defect centres in natural and HPHT diamond. The energy level positions and spins are listed for the ground state.

Labels	Model	Symmetry	ZPL (eV)	Position	Spin
A	$[N_S–N_S]^0$	D_{3d}	3.758, 3.902, 3.928	$E_C - 4$ eV	0
B	$[4N_S–V]^0$	T_d	—	—	0
C, P1	N_S^0	C_{3v}	—	$E_C - 1.7$ eV	1/2
B_S^0	B_S^0	T_d	—	$E_V + 0.37$ eV	1/2[a]
R2	I^0	D_2	1.685; 4.0	—	0[b]
R1	$[I–I]^0$	C_{1h}	—	—	1
GR1	V^0	T_d	1.673	$\sim E_C - 3.2$ eV	0
ND1, S1, S2	V^-	T_d	3.150	$\sim E_C - 3.2$ eV	3/2
TH5, W6/R4	$[V–V]^0$	C_{2h}	2.543	—	1
W15	$[N_S–V]^-$	C_{3v}	1.945	—	1
2.156 eV	$[N_S–V]^0$	C_{3v}	2.156	—	0
H2	$[2N_S–V]^-$	C_{2v}	1.257	$E_C - 2$ eV	1/2
H3	$[2N_S–V]^0$	C_{2v}	2.463	—	0

[a] For B_S^0 the sum of the electronic spin $S = 1/2$ and orbital momentum $L = 1$ gives a total magnetic moment $J = 3/2$ (Ammerlaan 1989).
[b] In fact, the R2 ESR centre corresponds to the excited $S = 1$ state of I^0 situated 50 meV above the ground $S = 0$ state.

or without an applied electric field (Fizgeer *et al* 2001, Konorova *et al* 1984, Cytermann *et al* 1994).

The absence of any significant post-growth diffusion of nitrogen at $T < 1500\,^\circ$C has been previously deduced from experiments on nitrogen aggregation (Evans and Qi 1982). Although no post-growth diffusion of elements larger than hydrogen has been reliably detected in diamond, there is no doubt about the occurrence of Si diffusion *during* the growth of CVD diamond (see section 5.4.7).

4. Basic defects in natural and HPHT diamond

4.1. Intrinsic defects

Some parameters of basic defects in natural and HPHT diamond are listed in table 1. The primary intrinsic defects in diamond are the vacancy and the ⟨100⟩-split interstitial (labelled as I). They may be created by irradiation, by heat or plastic deformation, or may just be inherent to the synthesis technique.

4.1.1. Isolated vacancy. The vacancy in diamond has been reliably identified only in its neutral (V^0) and negative (V^-) charge states, both states exhibiting T_d symmetry. The neutral vacancy has been associated with the GR1 optical centre, showing a ZPL at 1.673 eV in absorption, PL and CL, and with several more absorption lines in the 2.88–3.0 eV range, referred to as the GR2, GR3, ..., GR8 system. Photoluminescence excitation (PLE) measurements performed on the GR1 line showed that the GR1, GR2, ..., GR8 centres share a common ground state (Collins *et al* 1988a). This ground state is diamagnetic, but an excited $S = 2$ state of the V^0 centre has been detected (van Wyk *et al* 1995) by means of light-induced electron spin resonance (LESR). The negative vacancy possesses an $S = 3/2$ ground

state, which has been also characterized by means of ESR (Isoya *et al* 1992), and exhibits an absorption transition at 3.15 eV (the ND1 optical centre). The minimum temperature required to anneal out the vacancy (T_{an}) is believed to be independent of the vacancy charge state, but it varies with annealing time (Alekseev *et al* 2000). T_{an} is about 600 °C for a common few-hours-long annealing.

4.1.2. Vacancy-related complexes. In pure IIa diamond, isolated vacancies anneal out at ∼600 °C to form divacancies, associated with the TH5 absorption line and with the W6/R4 $S = 1$ ESR centre (Twitchen *et al* 1999a). Divacancies in turn anneal out at ∼800 °C, supposedly resulting in ⟨110⟩ chains of 3–7 vacancies (Lomer and Wild 1973) and other yet unidentified multivacancy complexes.

Annealing of single vacancies in type Ib and IaA diamonds leads to their capture by the C and A centres, resulting in the formation of N_S–V and $2N_S$–V complexes, respectively. The C centre captures vacancies about eight times more efficiently than the A complex (Iakoubovskii and Adriaenssens 2001). It is believed that the N_S–V and $2N_S$–V centres are stable against annealing at $T < 1400$ °C, and that at $T > 1400$ °C the N_S–V centres can aggregate into N_S–N_S and $2N_S$–V complexes (Collins 1979). However, interconversions between the $2N_S$–V and N_S–V centres have been observed after 1 h of annealing at temperatures as low as 1200 °C (Webb and Jackson 1995).

Two charge states are known for the N_S–V centre. The $[N_S–V]^-$ state has been thoroughly characterized by means of absorption, PL (Davies and Hammer 1976) and many varieties of ESR (He *et al* 1992, 1993a, b, Hanzawa *et al* 1993, Hiromitsu *et al* 1992, van Oort *et al* 1988, 1990, Redman *et al* 1991). It has C_{3v} symmetry, an $S = 1$ ground state, and exhibits a ZPL at 1.945 eV, which is not observable in CL.

A ZPL at 2.156 eV, detected in absorption, PL, and CL, has been attributed to the $[N_S–V]^0$ charge state on the basis of the photochromic behaviour, which was found to be complementary to that of the 1.945 eV line (Mita 1996, Iakoubovskii *et al* 2000a). An $S = 1/2$ ground state is expected for the $[N_S–V]^0$ centre, but it has so far eluded ESR detection (Baker and Newton 1995). Also, optical Zeeman measurements failed to resolve any splitting (<0.5 meV) for magnetic fields up to 43 T in the 2.156 eV PL line (Iakoubovskii 2000), which was interpreted as incompatible with the $S = 1/2$ $[N_S–V]^0$ model. Hence, an $S = 0$ $[N_S–V]^+$ alternative was proposed for the 2.156 eV centre. However, we want to remark here that if the respective g-factors for the ground and excited states are nearly equal and if the orbital contribution to the splitting can be neglected, then no Zeeman splitting is to be expected for an $S = 1/2$ centre. Consequently, Zeeman splitting results can hardly provide decisive evidence in favour of one or the other model for the 2.156 eV centre.

As to $2N_S$–V complex, two charge states are known. The neutral one has C_{2v} symmetry, an $S = 0$ ground state, and exhibits a ZPL at 2.463 eV (the H3 system seen in absorption, PL, and CL; Davies *et al* 1976). An excited $S = 1$ state of the $[2N_S–V]^0$ centre has been characterized by LESR (van Wyk and Woods 1995). A ZPL at 1.257 eV (H2 absorption and the PL system) has been ascribed to the $[2N_S–V]^-$ complex (Mita *et al* 1990, 1993). An $S = 1/2$ ESR spectrum has also been associated (Nisida *et al* 1992) with this complex; however, these ESR data seem inconclusive and may need additional confirmation (Newton 2001).

4.1.3. Carbon interstitials. Most interstitial-related *optical centres* in diamond exhibit a sharp vibronic peak of vibrational energy larger than the maximum phonon energy (165 meV or 1332.5 cm^{-1}), termed the local vibration mode (LVM). The LVM can be detected either directly in IR absorption or via electron–phonon transitions in UV–visible absorption, PL, or

CL. In isotopically enriched diamonds with comparable content of ^{12}C and ^{13}C isotopes, the LVM splits into several peaks (natural isotopic composition of C: 98.9% ^{12}C ($I = 0$); 1.1% ^{13}C ($I = 1/2$)). By analysing the splitting pattern one can deduce the number of atoms involved in the corresponding vibration. The presence of a LVM in optical spectra, though, may imply, but not guarantee, that the corresponding defect contains an interstitial: for one thing, the N_S^0 and $[2N_S{-}V]^-$ centres do not involve interstitials, but they do show LVMs at 1344 and 1348 cm^{-1}, respectively (Collins 1999). A characteristic ESR signature of an interstitial-related defect is strongly anisotropic hf interaction matrices and vanishing signals due to hf interaction with the nearest-neighbour carbon sites (Hunt *et al* 2000a). Those features originate from the p-like character of an unpaired electron in a split interstitial. Several carbon-interstitial-related optical centres have been characterized in irradiated natural and HPHT diamonds.

The isolated carbon interstitial has not been detected yet, even at the lowest temperatures achieved for diamond irradiation (4.2 K). There is an indication that it migrates, forming singly and multiply split interstitials, and impurity–interstitial complexes. Singly split, di-split, and possibly tri-split interstitials were identified by ESR and termed R2 (Hunt *et al* 2000a), R1 (Twitchen *et al* 1996), and O3 (Hunt *et al* 2000b) centres, respectively. Optical absorption from irradiated diamond persistently shows, along with the vacancy-related GR and ND1 lines, peaks at 1.685, 1.859, 4.0, and 2.463 eV. The first three lines are not active in luminescence; they have been associated with the singly ⟨100⟩-split interstitial (Davies *et al* 2000). Because of symmetry restrictions, the ⟨100⟩-split interstitial should also be inactive in IR absorption (Collins 1999). The above-mentioned 2.463 eV line belongs to the 3H centre, observed in absorption, PL and CL. Here, however, there appears an influence of nitrogen contamination: in nitrogen-containing diamonds the 3H absorption line is about 50 times weaker than the GR1 peak (Clark *et al* 1956, Davies *et al* 1992, Collins and Rafique 1979). However, the intensities of those peaks may be comparable in nitrogen-free diamond (Allers *et al* 1998).

As to the influence of heating, ESR and optical measurements reveal that the R1 and R2 ESR signals and the 3H, 1.685, 1.859, and 4.0 eV absorption lines anneal out in the temperature range 300–400 °C (Twitchen *et al* 2001, 1999b, Walker 1979). However, PL measurements show that a significant proportion of the 3H centres still remain present after annealing in the range 400–900 °C, only disappearing after annealing at $T \geqslant 1000$ °C (Iakoubovskii and Adriaenssens 2000a). The current (tentative) model pictures the 3H centre as a complex of two split interstitials separated by a lattice atom (Twitchen *et al* 2001).

4.1.4. Other interstitial-related centres, not involving nitrogen.

(a) The 5RL system, of C_{2v} symmetry about the ⟨100⟩ axis, exhibits a ZPL at 4.583 eV (absorption, PL and CL). Its LVM has the highest energy (237 meV) of all known defect centres in diamond. In diamond with comparable ^{12}C/^{13}C isotopic content this LVM splits into three lines, indicating that a pair of carbon atoms is involved in the vibration. Interestingly, the 5RL absorption strongly decreases upon annealing at 700 °C for 1 h (Collins and Spear 1986), but the 5RL CL spectrum disappears only upon annealing at 1000 °C for 1 h (Gippius *et al* 1983). Most parameters of the 5RL centre would comply with the ⟨100⟩ single-split-interstitial model. However, the high annealing temperature of the 5RL centre renders this assignment unlikely.

(b) The TR12 centre, characterized by a ZPL at 2.638 eV (absorption, PL, and CL), has C_{1h} symmetry and anneals out at 800–900 °C (Davies *et al* 1981, Gippius *et al* 1983). A LVM is observed at 200 meV: it does not split, but broadens for ^{13}C-enriched diamond, suggesting that several (∼6) carbon atoms are involved in the vibration (Mainwood *et al* 1994). Annealing of the single split interstitial correlates with the observed increase in the TR12 absorption (Allers *et al* 1998) confirming the interstitial nature of the TR12 centre.

The TR12 system is often accompanied by a weaker TR13 peak at 2.670 eV (Steeds *et al* 2000).

(c) Irradiation of IIa diamond produces a LVM peak at 1530 cm^{-1} observed directly in IR absorption. It anneals out at 300–400 °C giving rise to other LVM absorption peaks at 1570 and 1924 cm^{-1}, which in turn disappear upon annealing in the range 650–900 °C. Carbon and nitrogen isotope substitution studies reveal that the 1530 and 1570 cm^{-1} centres involve one carbon split interstitial, and that the 1924 cm^{-1} centre originates from a =C=C=C= chain (Collins *et al* 1988b).

4.2. Impurity related defects

4.2.1. Interstitial-related centres involving one nitrogen atom.

(a) The H1a centre is characterized by an IR absorption peak at 1450 cm^{-1}. On the basis of nitrogen and carbon isotopic substitution studies, combined with theoretical modelling of vibrational frequencies, it has been associated with the bond-centred nitrogen interstitial (Kiflawi *et al* 1996). This interstitial-related centre shows remarkable temperature stability: it anneals out only at ∼1500 °C, where the nitrogen aggregation is initiated.

(b) IR absorption peaks at 1706 and 1502 cm^{-1} can be produced by irradiation, followed by annealing at ∼400 and 700 °C, respectively. Isotopic substitution indicates that they both involve a C–N bond (Collins *et al* 1988b).

(c) Lines at 3.188 and 2.807 eV are observed in absorption, PL, and CL for irradiated Ib diamond. The 2.807 eV line is usually much weaker than the 3.188 eV peak. $^{15}N/^{14}N$ and $^{13}C/^{12}C$ isotopic substitutions indicate that both centres involve one substitutional nitrogen atom and one interstitial carbon atom, but originate from different defects (Collins and Lawson 1989). It was proposed that the 3.188 eV centre involves a carbon interstitial occupying a tetrahedral site next to a N_S atom (Zaitsev 2000). Similar to the H1a centre, the 3.188 and 2.807 eV systems remain stable against annealing at temperatures up to 1500 °C (Gippius *et al* 1983).

(d) Absorption lines at 2.086, 2.917, and 1.77 eV are commonly observed in irradiated Ib diamond. They are thought to contain an interstitial atom because of their annealing behaviour: annealing of vacancies does not affect the intensity of those three centres, but all of these disappear upon annealing at ∼900 °C for 1/2 h (Nisida *et al* 1989). There is evidence that the 2.917 and 2.086 eV lines share a common ground state and, therefore, belong to the same defect (Davies and Nazaré 1980).

(e) Absorption lines at 1.979 and 2.367 eV probably originate from different orientations of a defect involving a substitutional nitrogen and two interstitial carbon atoms (Collins and Rafique 1979). The defect anneals out at ∼200 °C.

4.2.2. Some other impurity-related centres. The N_S centre is one of the most studied centres in diamond. In the neutral charge state (N_S^0 or P1 or C) it is a deep donor with the ground state at $E_C - 1.7$ eV. This charge state has been thoroughly characterized by means of ESR, photoconductivity (PC), and IR and UV–visible absorption. The ESR reveals that the nitrogen atom in N_S^0 is shifted off-centre, resulting in C_{3v} symmetry. The IR absorption spectrum associated with N_S^0 contains a dominant broad line at 1130 cm^{-1}, which is routinely used to determine the N_S^0 concentration (Davies 1999), and a sharp LVM peak at 1344 cm^{-1}.

The IR spectrum from the N_S^+ charge state, showing a prominent peak at 1332 cm^{-1}, was identified by ionizing the N_S^0 centres with UV light (Lawson *et al* 1998). Unfortunately, the value 1332 cm^{-1} corresponds to the Raman frequency in diamond. IR absorption at

this wavenumber can be induced in a perfect diamond lattice by an applied electric field (Anastassakis and Burstein 1970) or by the presence of tetrahedral defects, such as B_S, $4N_S$–V (the B centre), N_S^+, etc (Walker 1979). This obfuscates unambiguous detection of N_S^+ by IR absorption. Meanwhile, the luminescence and UV–visible absorption signatures of this non-paramagnetic defect are not known yet. An absorption and PC threshold at ∼2.2 eV (No 7 in figure 1, which will be described later) has been attributed to an electron transition from the ground state of N_S^0 to the conduction band. A PC threshold at ∼4.6 eV, which is absent in absorption spectra, has been assigned to the electron transitions from the valence band to the N_S^+ (Iakoubovskii and Adriaenssens 2000b). The main part of a broad absorption peak centred at ∼4.6 eV (label 8 in figure 1; see later) originates from electron–phonon transitions at a trigonal centre with a ZPL at 4.059 eV. This centre was first identified with N_S^0 (Nazaré and Neves 1987). Later, an anti-correlation was found between the intensities of the 4.6 eV absorption band and both the IR and visible absorption signals from N_S^0, suggesting that N_S^0 is not responsible for the 4.6 eV feature. Instead, the latter was tentatively ascribed to the neutral B_S–N_S pair (Iakoubovskii and Adriaenssens 2000b).

Analysis of vibration frequencies shows that an IR absorption line at 3107 cm^{-1}, observed in natural and HPHT diamonds, originates from a C=CH_2 group. This species probably occurs in voids rather than in the bulk of diamond (Davies *et al* 1983).

Only one PL and absorption system with a ZPL line at 1.682 eV has been reliably associated with Si doping in as-grown HPHT crystals. However, after the samples were electron irradiated and annealed at $T > 600\,^{\circ}C$, a series of Si-related absorption lines at 1.679, 1.682, 1.691, and 1.711 eV emerged (Kiflawi *et al* 1997).

4.3. Broad-band (band-A) luminescence.

Most PL and CL spectra in any type of diamond are dominated by broad (∼0.5 eV width) signals. They are often referred to as band-A emission, although this term clearly needs further specification as numerous distinctly different broad emission bands exist in diamond. They appear poorly reviewed in the literature, despite many being frequently observed for CVD diamond. Therefore, in this section, the dominant broad luminescence bands in diamond are overviewed in more detail. They are listed according to their peak energy.

Obviously, a broad band can be generated via strain-induced broadening from a vibronic sideband of almost any ZPL. Such situations will not be considered here unless the strain is intrinsic to the defect (see, e.g., item (4) below). Besides these, however, there exist broad luminescence signals in diamond, which do not show any resolved structure in any sample studied so far. It was suggested that they could all be explained by the donor–acceptor (DA) pair recombination model (Dean 1965). This predicts that the energy of luminescence from a DA pair, separated by a distance r, is $h\nu(r) \sim E_g - (E_D + E_A) + e^2/\varepsilon r$, where $E_g = 5.47$ eV is a band-gap width, E_D and E_A are the ionization energies of the donor and acceptor, respectively, e is the electronic charge, and ε is the static dielectric constant. Because of the discrete nature of the distance r, narrow emission peaks would be expected in this model. Their absence, though, in most DA bands in diamond was attributed to the strong electron–phonon coupling at deep donors or acceptors involved in recombination. Differences in the position of the maxima of broad bands were ascribed to variations in the distribution of the DA separation distance r from sample to sample. Obviously, r cannot be smaller than some value r_{min} (∼2 Å for diamond), and a more complex expression is required for $h\nu(r)$ when r is approaching r_{min}. From the typical width of the broad bands in diamond the peak position for the DA pair recombination can be roughly estimated as $E_g - (E_D + E_A) + 0.5$ eV.

The DA model successfully explained some features of broad emission bands in diamond, such as the variations in the shape and intensity of some spectra with temperature and excitation energy. However, as might be expected, a unified origin can hardly exist for *all* broad emission bands in diamond. Another problem the model faces is in finding appropriate donors and acceptors. B_S^0 and N_S^0 are the most abundant acceptor and donor centres, respectively, in diamond. Yet, taking their ionization energies as 0.37 and 1.7 eV, respectively (Walker 1979), the luminescence peak position in the DA recombination model can be estimated as ∼3.9 eV—a value that suits almost no broad luminescence band in diamond. Indeed, many signals with other peak energies and of origin other than DA are observed, as discussed below:

(1) The IR luminescence band observed at ∼1.2 eV in Ia diamond was associated with planar ⟨100⟩ defects of unknown structure, called platelets, by direct high-resolution microscopical observations (Wight *et al* 1971). PLE measurements suggest it to originate from radiative recombination between two bands of electronic states separated by a gap of ∼1.7 eV (Iakoubovskii and Adriaenssens 2000c).

(2) Some HPHT diamonds show a broad PL band peaking at 1.85 eV. This band was tentatively ascribed to DA recombination based on its relaxation behaviour. The 1.85 eV PL competes with the broad signal centred at 2.3 eV (see (4) below) and therefore, it was proposed that those bands share a common donor or acceptor (Klein *et al* 1995).

(3) HPHT diamonds with uncompensated boron acceptors show phosphorescence bands peaking at 2.1, 2.45, and 2.6 eV. The temperature dependences of the phosphorescence intensity suggest that all these signals involve boron acceptors and originate from DA recombination (Watanabe *et al* 1997, Fujita *et al* 1996).

(4) Most HPHT and some natural diamonds, as well as most CVD diamond films, show a broad green band at ∼2.3 eV. PLE measurements reveal that in most CVD samples it consists of two signals, labelled green bands I and II (Iakoubovskii and Adriaenssens 2000d). The green band I is specific to CVD films and it is attributed to recombination within the amorphous carbon (a-C) phase (Iakoubovskii and Adriaenssens 2000d). The green band II is observed in all types of diamond. Analysis of its PL relaxation behaviour (Klein *et al* 1995), and PLE (Iakoubovskii and Adriaenssens 2000d) and ODMR (Nazaré *et al* 1995) spectra suggests that this band originates from DA recombination. The intensity of the green band II correlates with the concentration of B_S defects (Lawson *et al* 1995, Collins 1992, 1993) and, therefore, it is widely believed that B_S is the acceptor in the corresponding DA recombination model. The green band II could be produced in natural IIb diamond with low nitrogen content (<0.1 ppm) by neutron irradiation, followed by annealing at 800 °C for 2 h (Iakoubovskii *et al* 2001). This fact was interpreted as evidence for a structural (irradiation-induced) defect being involved in the DA recombination. PLE spectra for the green band II show a threshold at 3.2 eV. The ODMR reveals that N_S^0 is involved in the DA recombination: by monitoring PL from the green band II, the N_S^0 (P1) ESR spectrum was recorded.

At least two DA models can be considered for the green band II. The first one assumes B_S as the acceptor and a structural defect as the donor. The 3.2 eV PLE threshold should then correspond to electronic transitions from the valence band to the donor level ($E_V \rightarrow E_V + 3.2$ eV). However, this threshold is observed in synthetic Ib diamond, where the Fermi level should be pinned at $E_C - 1.7$ eV by the N_S^0 defects. So, in order to make such transitions possible, inhomogeneities in the Fermi level position should be present. The ODMR spectrum of the green band II is explained within this model as the N_S^0 donors are not directly involved in the DA recombination, but rather act as quenching centres. A possible mechanism is that the electrons (holes) from the donors (acceptors) involved into

the green band II tunnel to the N_S^0 centres, thus changing their occupations and inducing the ODMR signal. The presence of quenching centres is consistent with the PL relaxation results. The absence of signals from the donors and acceptors in ODMR spectra can be explained as follows as to the acceptor, in this model the presumed acceptor is B_S. This shallow centre shows a strong spin–orbit (SO) coupling and thus may remain undetected due to excessive line broadening of the corresponding ESR signals (Ammerlaan 1989). The non-observation of the donor, however, is less clear. A possibility here is that the electrons from the donors are quickly transferred to the N_S^0 and, should their lifetime there be long enough, one would expect the ODMR signals from the donors to be much weaker than from the N_S^0 centres, in accordance with ODMR results.

In the second model the N_S^0 acts as the donor and a structural, possibly boron-containing, defect as the acceptor A. This model naturally explains the 3.2 eV PLE threshold in terms of ionization of A^- resulting in the production of A^0, the latter being involved in the DA recombination. Because of the deep-centre relaxation, the ground-state position of A^0 may then be situated below the $E_C - 3.2$ eV level. Given the N_S^0 level at $E_C - 1.7$ eV, the acceptor ground state should be situated at $\sim E_C - 3.5$ eV in order to produce a band centred at $\sim$2.3 eV. The presence of the N_S^0 signals in the ODMR spectra is obviously accounted for by the second model. However, a weak point in this model is that a deep acceptor involved into the DA recombination should then have insignificant SO coupling with the valence band (reduced line broadening) and show an $S = 1/2$ ODMR signal, which has not been detected yet. Additional assumptions, such as, e.g., stress broadening, large g-anisotropy and short recombination lifetime, are required to explain this non-observation. Though it may appear that the second model for the green band II requires fewer assumptions than the first one, no unambiguous proof in favour of either model has been obtained yet.

A series of papers by Hayashi *et al* (1996) reported that the 2.3 eV band in CVD diamond could be repeatedly enhanced by H_2 plasma treatments and then bleached by O_2 plasma. This was considered as evidence for a hydrogen-related nature of the green band II. However, similar results were obtained by exposure of CVD diamond to air followed by vacuum annealing at 400 °C for 2 h. Therefore, those variations in the intensity of the green band II were attributed to changes in the Fermi level position due to the surface hydrogenation and dehydrogenation (Iakoubovskii and Adriaenssens 2000d). It is possible that the Fermi level shift is the reason for the observed increase in the 2.3 eV band intensity with boron doping and that boron atoms are not involved in the defects responsible for the green band II at all.

(5) Almost any natural IIb, IIa, Ib, or CVD diamond shows a broad luminescence band centred at $\sim$2.8 eV. Spatial measurements of the blue emission using an electron microscope revealed that it originates from dislocations (Yamamoto *et al* 1984). Its intensity does not correlate with nitrogen or boron doping (Ruan *et al* 1992). On the basis of previous microscopical results combined with PLE measurements it was suggested that the 2.8 eV band concerns a vibronic sideband of some dislocation-related defect centre, which is broadened by strain around the dislocations (Iakoubovskii and Adriaenssens 2000d).

(6) Most Ia diamonds show a broad blue luminescence band at 3 eV. Despite their large width ($\sim$0.4 eV), there is a distinct peak position difference between the 3 and 2.8 eV bands. No evidence has been reported that the 3 eV band originates from dislocations and no model for this band appears to exist yet. In contrast, in inhomogeneous natural diamonds the origin of the blue emission appears to be dislocations in the IIa regions, but not so in the Ia areas (Kiflawi and Lang 1974).

(7) There is a boron-related broad *luminescence* band at 4.6 eV, which, however, is not related to the 4.6 eV absorption band discussed in section 4.2.2: the former is seen in CL from boron-doped HPHT and CVD diamond, and in B^+-implanted natural IIa crystals (Lawson *et al* 1995, Sternschulte *et al* 1996), while the latter is only detected in absorption, in diamonds containing uncompensated nitrogen. There is one more broad emission band at 4.6 eV, which is observed in phosphorus-doped CVD diamond (Koizumi *et al* 2001).

5. Defects in CVD diamond

5.1. CVD diamond growth: some salient aspects

The majority of CVD diamond films produced nowadays are nominally undoped polycrystalline layers of <100 μm thickness, with random or almost random orientation of the grains. Most of them are grown from a $\sim 1:99$ CH_4:H_2 gas mixture, on a Si substrate kept at a fixed temperature in the range 700–900 °C. In most CVD reactors, however, there are unavoidable air leaks. Also, the growth may occur in ambient atmosphere (e.g., in torch CVD) (Pan and Kania 1995). So, there may be present a significant number of O_2 and N_2 molecules in the feed gas.

The CVD synthesis requires a plasma which etches all materials it is in contact with: the substrate, which is typically Si or, occasionally, metals or diamond; the substrate holder (typically Mo); the chamber walls (steel or Al); the windows (silica); the spiral in hot-filament CVD (W, Ta, or Re); etc. All these elements can be ionized by the plasma and may thus be introduced into the diamond film. Furthermore, the CVD growing surface is continuously bombarded by plasma particles; the synthesis itself is fast and has a non-equilibrium nature. Consequently, vacancies and interstitials are continuously produced in growing CVD diamond, and they may be considered as inherent to the CVD process. Some of the above peculiarities of the synthesis strongly affect the physical properties of CVD diamond films. They contain metallic inclusions in addition to considerable amounts of H, O, Si, N impurity (Zhou *et al* 1996, Dollinger *et al* 1995, Iakoubovskii *et al* 2000b).

As mentioned, ESR signals from CVD samples with randomly oriented grains exhibit a specific shape called a 'powder pattern' (see, e.g., figures 3 and 4, later), limiting information on defect symmetry. Unfortunately, determination of the defect symmetry in such CVD samples by optical techniques is hardly possible: samples are thin and strongly scatter light. Consequently, absorption in these films is small and is often difficult to measure correctly.

However, deviations from the above 'standard' sample conditions may imply:

- Films can be grown, albeit at reduced quality, at temperatures as low as 200 °C (see, e.g., Hiraki 2000) and as high as 2100 °C (Iakoubovskii *et al* 2000c)
- The film thickness can be as large as a few millimetres. However, then most manufacturers, largely for commercial purposes, make special efforts to reduce the impurity content. The resulting films are of very good quality (the so-called optical window quality), showing almost no absorption in the visible–UV range.
- By choosing a proper substrate material (diamond) and/or special growth conditions, monocrystalline or highly oriented CVD samples can be prepared.
- Films can be doped by introducing an extra feed gas or a solid into the growth chamber, e.g., N_2, O_2, H_2S, PH_3, B_2H_6, P_2O_5, B_2O_3.

It is interesting to combine the knowledge of the properties of basic defects in natural and HPHT diamonds with information on the CVD growth conditions, and try to predict what

defects could be present in CVD diamond. Because of the relatively high growth temperatures of CVD diamond, the isolated vacancies and interstitials should not be observed, but, given the impurities present, complexes of vacancies with H, N, O, Si, and other impurities are anticipated. So, hydrogen–vacancy, oxygen–vacancy, and Si–vacancy complexes may be specific to CVD diamond, in contrast with the natural and HPHT diamonds, as bulk H, Si, and possibly O impurities are not abundant in the latter. Luminescence from the interstitial-related 5RL, TR12, 3H, 3.188, and 2.807 eV centres is expected. Interstitial-related absorption lines at 1502, 1570, 1706, and 1924 cm^{-1}, and at 1.77, 2.086, and 2.917 eV can be present as well, but they may still remain undetected due to the low sensitivity of absorption measurements. Because the CVD growth temperatures are too low for nitrogen aggregation to occur, one would expect to see defects containing one nitrogen atom, but not complexes. Reassuringly, most of the above 'predictions' appear to be borne out, as discussed below.

5.2. Centres related to interstitials or vacancies

Indeed, luminescence spectra typically show the 5RL, 3.188, and 2.807 eV systems in as-grown CVD diamond (Partlow *et al* 1990, Sternschulte *et al* 1996, Lin *et al* 1996, Collins *et al* 1989, etc). The 3H centre has also been detected by means of PL in as-grown CVD films (Iakoubovskii and Adriaenssens 2000a). Yet, there are few reports on reliable observation of the carbon interstitial TR12 centre in CL from as-grown CVD diamond (Ruan *et al* 1991, Collins *et al* 1989). However, in most CVD films, instead of TR12 (C_{1h} symmetry, the ZPL at 2.638 eV, and the LVM at 200 meV, $T_{an} = 800$–$900\,^{\circ}C$), a very similar spectrum, labelled TR12′, is observed (Iakoubovskii and Adriaenssens 2000a, 2000d, Rzepka *et al* 2001). TR12′ has C_{1h} symmetry, the ZPL at ∼2.65 eV, the LVM at 220 meV, and a weaker satellite (TR13′) at 2.675 eV. The position of the TR12′ ZPL can vary in the range 2.648–2.654 eV, even within one sample, probably due to strain. The TR12′ spectrum is stable up to at least 2100 °C and it is probably not nitrogen related (Iakoubovskii and Adriaenssens 2000a). In order to explain all these features, it was proposed that TR12′ is TR12 trapped by an impurity, possibly oxygen. No absorption signals from interstitial-related centres in CVD diamond have been reported yet.

As to vacancy-related defects, only one paper is known to have reported on a reliable CL observation of the isolated vacancy (GR1, with the ZPL at 1.673 eV; see table 1) in as-grown CVD diamond (Allers and Mainwood 1998). In early luminescence studies of CVD diamond, the GR1 peak was often confused with Si-related PL lines at 1.682 and 1.679 eV, which will be discussed later. In the study by Allers and Mainwood, the GR1 and Si-related CL lines could be spectrally resolved and discriminated. By changing the incident electron energy, a depth scanning in the range 0–10 μm was performed. It revealed that the concentration of neutral vacancies rapidly increases towards the surface. Accordingly, it was suggested that the observed vacancies are those generated during the last minutes of the growth process: they are exposed for a relatively short time to high temperature and could therefore survive. Unfortunately, no information on the growth conditions of the films studied could be provided.

Here, it may appear relevant to add that in the course of the study of nitrogen incorporation in homoepitaxial CVD diamond films (see section 5.4.4), the authors of this review encountered an unusual fact: films grown at temperatures as high as 2100 °C for >10 h exhibited strong ESR signals originating from the interstitial-related R1 and R2 centres. However, post-growth annealing at 600 °C for 1 h removed those signals. Along with the results discussed above, this observation reveals that defects, such as isolated vacancies and split interstitials, normally unstable at the high temperatures of CVD diamond synthesis, can be created in CVD diamond during the last minutes of the fierce growth process.

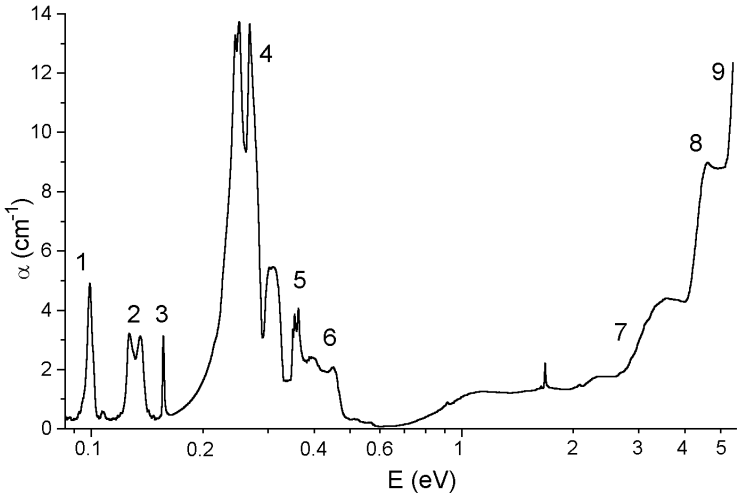

Figure 1. The room temperature photon absorption spectrum of a nominally undoped as-grown CVD diamond film, where α is the absorption coefficient. Note the logarithmic x-axis scale. The spectrum has been roughly corrected for light scattering by subtraction of a quadratic parabola.

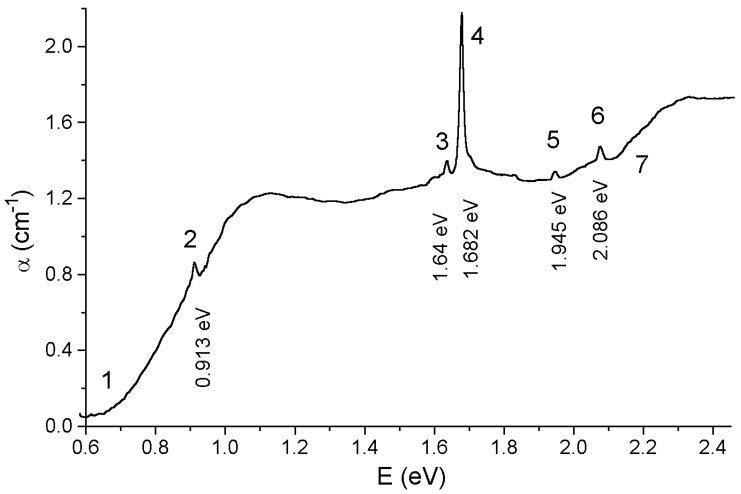

Figure 2. A detailed view of the 0.6–2.4 eV spectral region shown in figure 1.

Figure 1 presents a room temperature absorption spectrum from a nominally undoped as-grown CVD diamond film. In order to show IR and UV peaks in one graph, a logarithmic x-scale has been used. Parts of this spectrum, however on different scales, have been reported earlier (Iakoubovskii and Adriaenssens 2000b, 2000e, 2001). Labels 4, 6, and 9 in figure 1 indicate intrinsic diamond features: two-phonon, three-phonon, and band-to-band absorption, respectively. A magnification of the 0.6–2.4 eV spectral region from figure 1 is shown in figure 2. It reveals narrow lines at 0.913, 1.640, 1.682, 1.945, and 2.086 eV. The 1.945 and 2.086 eV peaks may be identified with the $[N_S–V]^-$ and the interstitial-related 2.086 eV centres, respectively, which were discussed in sections 4.1.2 and 4.2.1.

Figure 3 shows a selected ESR spectrum from an as-grown CVD diamond film (Q-band, 300 K). The central part of the spectrum is expanded in figure 4. Although the sample used

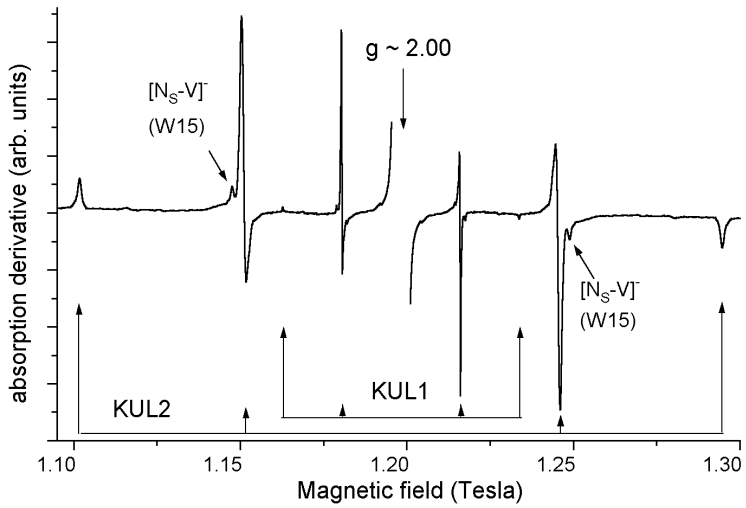

Figure 3. The first-derivative ESR spectrum observed for as-grown CVD diamond film under the following conditions: $T = 300$ K; $f \sim 34$ GHz; cavity Q-factor: ∼1500; incident microwave power: ∼1 μW; modulation amplitude: 0.3 mT. The strong signals at $g \sim 2$ are removed and shown in figure 4.

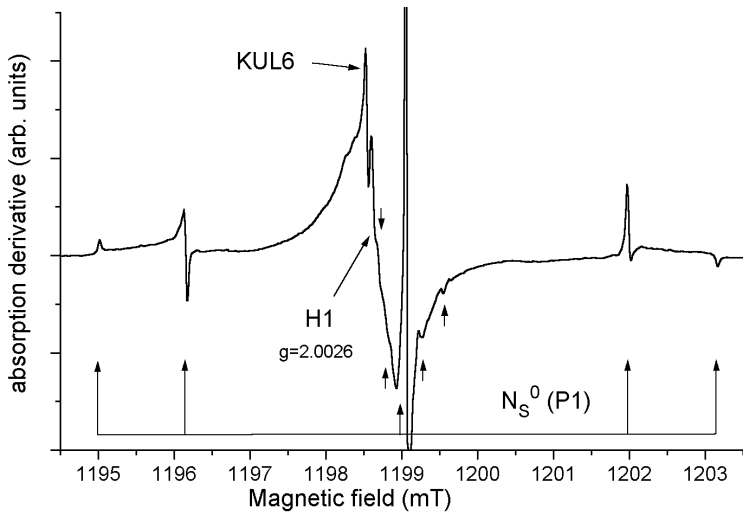

Figure 4. The central part (around $g \sim 2$) of the ESR spectrum shown in figure 3 measured under the same spectroscopic conditions, except for applying a lower modulation amplitude (0.03 mT). Short arrows mark the ^{13}C hf lines belonging to the P1 centre.

for figures 3 and 4 was nominally undoped, nitrogen-related P1 (N_S^0) and W15 ($[N_S–V]^-$) signals are seen. Integration of the spectrum yielded concentrations of ∼8 ppm for the P1 and ∼0.1 ppm for the W15 centres.

5.3. Defects related to other structural imperfections

There are several gross features dominating almost any absorption, PC, luminescence, and ESR spectrum from CVD diamond, which can be attributed to structural defects. One of them, the green band I, was already mentioned in item (4) of section 4.3. There exists a linear correlation between the integrated intensity of the green band I and the intensity of a-C-related Raman signals (Bergman *et al* 1994). In their work, Bergman *et al* proposed to assign this band to the a-C inclusions in CVD diamond. This proposal was later confirmed by the observation of a *spatial* correlation between the green PL and a-C Raman peaks, and by the analysis of the polarization properties of the green PL (Iakoubovskii and Adriaenssens 2000d).

Another prominent feature, which is observed in photocapacitance (Zeisel *et al* 1999a), absorption (Nesladek *et al* 1996, Sharda *et al* 2001) and PC (Gonon *et al* 1994, 1995, Rohrer *et al* 1996, Rossi *et al* 1997, Nesladek *et al* 1998) spectra of CVD diamond, concerns a threshold at 0.7–0.9 eV. This threshold is also evident from the absorption spectra shown in figure 2 (label 1), and it was also found to be present in PC spectra measured on the same sample (Iakoubovskii and Adriaenssens 2000e). Moreover, a similar threshold can be produced in PC spectra of pure IIa or IIb diamond by plastic deformation (Samsonenko *et al* 1978) or by electron irradiation (Vermeulen and Halperin 1981). Therefore, it appears plausible to suggest that a structural defect is responsible for this feature. As the threshold is observed in boron-doped samples, where the Fermi level is pinned at $E_V + 0.37$ eV (Zeisel *et al* 1999a), it may be attributed to electron transitions from the valence band to a disorder-broadened level at $E_V + (0.7 \ldots 0.9)$ eV.

All published ESR spectra measured on CVD diamond exhibit a rather broad central Zeeman signal (see, e.g., figure 4) with a peak-to-peak linewidth of 0.2–0.5 mT and corresponding defect ($S = 1/2$) density of 10^{16}–10^{20} spins cm^{-3} (Zhou *et al* 1996). Before further addressing the nature of the originating defect, it may appear appropriate to insert a remark on the assigned g-value, or more broadly, on g-value determination practice in ESR work on diamond in general. The reported position of the broad line ($g = 2.0028$), as well as of most other ESR centres in diamond, is commonly determined relatively to the N_S^0 (P1) centre, of which the isotropic g-value was early on inferred as $g = 2.0024$ (Smith *et al* 1959). The ubiquitousness, stability, and favourable ESR properties of this defect, such as its narrow linewidth and its temperature-independent position, make it serve as a most convenient, almost natural spectroscopic g-value reference. However, recent upgraded calibration has yielded a modified g-value for the P1 centre as $g = 2.002\,16(1)$ and a zero-crossing g-value of $2.002\,17(1)$, the difference originating from the second-order (^{14}N hf interaction) corrections (Iakoubovskii and Stesmans 2001). Accordingly, all g-values mentioned in this article (see table 2) will appear a factor of $\sim 2 \times 10^{-4}$ smaller than in the literature, thus positioning the above-described broad signal at $g = 2.0026$.

It was concluded that when the above broad central Zeeman signal is observed to be flanked by two weaker, symmetrically positioned satellites, the total spectrum should originate from the $[H–V]^0$ defect (see section 5.4.1). However, the required satellites are frequently not present (see, e.g., Talbot-Ponsonby *et al* (1998)), and then the $g = 2.0026$ signal matches the one attributed to a carbon dangling bond. The latter can be observed in diamond heavily damaged by plastic deformation (Samsonenko *et al* 1978), crushing (Bell and Leivo 1967), or ion irradiation (Isoya *et al* 1997a), or in a-C (e.g., Zeinert *et al* (2000)). This overlap complicates the interpretation of the signal's origin. As to possible correlation with optical results, it may be possible that the $g = 2.0026$ ESR signals and the 0.7–0.9 eV absorption threshold originate from the same defect.

IR spectra from many CVD films show a characteristic one-phonon absorption spectrum (peaks 1, 2, and 3 in figure 1). Its intensity remains unchanged by annealing at 1000 °C for 2 h and is observed to increase about three times upon annealing at 1400 °C for 2 h. A very similar spectrum could be produced in pure IIa diamond by neutron irradiation and, consequently, it was concluded that it originates from an intrinsic defect(s) (Iakoubovskii and Adriaenssens 2001, 2002). The spectrum can grow particularly strong, much stronger than the diamond two-phonon absorption one, in thin, poor-quality CVD films (Kweon *et al* 2001, Iakoubovskii and Adriaenssens 2002). Such exceptional strength would be more typical for an organic group attached to the diamond lattice than for a point defect in it. However, the spectrum can also be produced by irradiation in pure diamond. Therefore, it is concluded that the spectrum may originate from sp^2 carbon-related species.

Another one-phonon IR absorption spectrum, common for as-grown undoped CVD films, is shown in figure 4 of the review by Zaitsev (1998).

5.4. Impurity-related centres

Impurities in diamond are ordered in this section according to their appearance in the periodic table. They can also be classified into: (1) impurities intrinsic to the CVD process, such as H, O, N, and Si (see section 5.1); and (2) (one hopes) electrically active dopants introduced intentionally, such as Li, B, S, and P. As for the latter, boron is known to be a reliable and controllable p-type dopant in all types of diamond. Realizing n-type doping of diamond is still a challenging physical and technological problem, for which a wide range of elements have been tried. However, only results obtained with Li, S, and P seem successful.

5.4.1. Hydrogen, the dominant impurity in CVD diamond. In order to determine the total concentration of an impurity in diamond, one commonly uses elemental analysis techniques, such as combustion analysis, SIMS, ERD, and NAA. Results obtained with those techniques must be treated with caution, as the methods applied are sensitive to obfuscation by occasional contamination (inclusions) by foreign substances in the sample studied and in the measurement environment. Special attention should be paid to hydrogen and oxygen, as they are involved in most contaminating substances. As an illustrative example, we may consider the determination of the dominant impurity in *natural* diamond by combustion analysis: the dominant impurity was initially suggested to be nitrogen (Kaizer and Bond 1959) and later oxygen (Melton and Giardini 1976). IR absorption studies of nitrogen aggregation were able to confirm that the nitrogen content determined by combustion analysis does indeed pertain to the bulk properties, because IR calibration constants themselves could be independently ascertained by analysing the nitrogen transformation between the A, B, and C centres. Meanwhile, no clear oxygen signature was observed in IR absorption. Therefore, it was concluded that nitrogen, unlike oxygen, is a dominant impurity in the bulk of natural (and HPHT) diamond, and oxygen is probably mostly concentrated at the surfaces, voids, and inclusions (see, e.g., Walker (1976)).

The above discussion of the oxygen contamination in natural diamond similarly applies to hydrogen in CVD diamond as well. Its total concentration, determined by means of nuclear magnetic resonance (NMR), ERD, or SIMS, is typically in the range 0.01–2 at.% (Zhou *et al* 1996, Stiegler *et al* 1998, Dollinger *et al* 1995). Most CVD films show IR absorption originating from different C–H bonds. Interestingly, the 3107 cm^{-1} hydrogen-related IR peak is frequently seen for natural diamond, but it has never been reported for CVD diamond. Instead, polycrystalline CVD films show a variety of absorption lines in the range 2800–2950 cm^{-1} (e.g., like features No 5 at around 0.36 eV in figure 1), while peaks at 3123.6 and 3323 cm^{-1} are observed for monocrystalline or highly oriented CVD diamond (Fuchs *et al* 1995). The

dominant lines in the range 2800–2950 cm^{-1} are identical to those produced by stretching vibrations of CH_2 and CH_3 groups in organic compounds and the hydrogen content in them can be estimated using organic standards (Haque *et al* 1998, Stiegler *et al* 1998). It was believed that IR-active hydrogen makes up only a small part of the total amount of hydrogen present in CVD diamond. However, combined IR and ERD measurements performed on the same samples indicate that the two techniques may arrive at similar results regarding the hydrogen content reaching a level of ∼2% (Stiegler *et al* 1998, Jubber and Milne 1996, etc). It is clear, though, that organic CH_2 and CH_3 groups are not relevant to the bulk of diamond. Also, it is hard to envision that 2% of hydrogen could be accommodated inside the CVD diamond grains without converting diamond into an amorphous-like structure. We, therefore, believe that most of the hydrogen detected by means of IR *vibrational* absorption, NMR, or elemental analysis techniques is present at the surface of CVD diamond; this hydrogen will not be considered any further here. Finally, it may be worth noting that the deformation vibrations of the CH_X groups produce a series of absorption peaks at 1300–1470 and 700–900 cm^{-1}, a fact that should be taken into account when analysing one-phonon spectra in CVD diamond.

Another notorious manifestation of the presence of hydrogen in CVD diamond is hydrogen-related surface conductivity. It is very well known that as-grown CVD films or diamonds, treated in hydrogen plasma after growth, exhibit conductive (∼100 kΩ cm) surface layers. Extensive work is currently being done on this phenomenon within the field of device and surface sciences. The current opinion is that the surface hydrogenation is a necessary but not a sufficient condition for establishing high surface conductivity; however, it has been found that adsorption of water at the surface is an essential aspect and the hydroxyl ions play an important role in this surface conductivity (Maier *et al* 2000). Consequently, this phenomenon will not be considered here either, being irrelevant to the bulk of diamond.

Nevertheless, hydrogen still appears as one of the dominant impurities in the bulk of undoped CVD diamond. Evidence for this comes from ESR measurements: as already indicated, the above-mentioned (section 5.2) signal at $g = 2.0026$, related to carbon dangling bonds, often exhibits two satellites—the spectrum ascribed to an $S = 1/2$ centre called H1. The spacing between satellite lines increases linearly with the microwave frequency f and their intensity decreases as $1/f^2$. Consequently, in the high-frequency ESR spectra the satellites can only be seen upon magnification of the spectrum (not shown in figure 4). It has been demonstrated that the satellites originate from the forbidden ($\Delta m = 1$) hydrogen hf transitions and that the central line is broadened due to unresolved allowed ($\Delta m = 0$) *anisotropic* hydrogen hf lines (Zhou *et al* 1996). Pertinently, for CVD samples with preferential orientation of the grains, the H1 ESR spectrum is perfectly isotropic. Therefore, in the absence of any apparent anisotropy, it was proposed that the H1 centres reside in the highly disordered near-surface regions of CVD films. However, theoretical modelling suggests a clear microscopic model for this ESR centre as a hydrogen atom trapped in a neutral diamond vacancy ($[H–V]^0$), and, therefore, this defect should rather be considered as a bulk one. Calculation also reveals that addition of a second hydrogen atom to the H–V centre is energetically unfavourable (Zhou *et al* 1996). This provides a plausible explanation for the fact that this dangling-bond-related defect is formed in high concentrations in diamond grown in hydrogen-rich ambient. Concentrations of H1 centres in the range 0.1–500 ppm have been reported (Zhou *et al* 1996, Talbot-Ponsonby *et al* 1998), making it a dominant bulk defect and, correspondingly, suggesting hydrogen to be a dominant bulk impurity in CVD diamond. Annealing study of the H1 centre (Talbot-Ponsonby *et al* 1998) provided information on the stability of the bulk C–H bonds in diamond. The intensity of the H1 ESR signals starts to decrease upon annealing at ∼1300 °C for 4 h, and disappears upon annealing at ∼1600 °C.

Table 2. Some parameters of the ESR centres (300 K) detected in CVD diamond (Zhou *et al* 1996, Iakoubovskii and Stesmans 2001). C is the maximal observed concentration.

Label	S	g_1	g_2	g_3	C (ppm)	Proposed model
P1	1/2	2.002 16(1)	2.002 16	2.002 16	100	N_S^0
H1	1/2	2.002 6(1)	2.002 6	2.002 6	500	$[H–V]^0$
H2	1/2	$\sim$ 2.003	$\sim$ 2.003	$\sim$ 2.003	0.5	
KUL1	1	2.004 1(1)	2.003 5	2.003 5	0.5	
W15	1	2.002 6(1)	2.002 6	2.002 6	1	$[N_S–V]^-$
KUL2	1	2.002 6(1)	2.002 6	2.002 6	10	$[H–2V]^-$
KUL3	1/2	2.005 03(5)	2.004 25	2.002 54	0.5	
KUL4	1/2	2.004 58(5)	2.003 15	2.002 58	0.5	
KUL5	1/2	2.002 90(3)	2.002 90	2.002 90	1	
KUL6	1/2	2.003 06(3)	2.002 91	2.002 91	1	

The spectroscopic parameters of another hydrogen-related ESR spectrum, labelled H2 (note that it has no relationship to the *optical* H2 centre discussed in section 4.1.2), are very similar to those of H1, except for the smaller linewidth of the former. The H2 centre is present in smaller densities and is much less frequently observed than H1 (Zhou *et al* 1996, Talbot-Ponsonby *et al* 1998).

Three more hydrogen-related ESR centres, labelled KUL2, 3, and 4, have been reported recently (Iakoubovskii and Stesmans 2001). KUL2 is an $S = 1$ centre characterized by isotropic $g = 2.0026$ and $D = 96.5$ mT, and is shown in figure 3. It appears always accompanied by the W15 centre ($g = 2.0026$, $D = 102.7$ mT), whose structure, i.e. $[N_S–V]^-$, has been previously determined from ESR studies of natural and HPHT diamonds (Loubser and van Wyk 1978). The intensity of both signals in CVD diamond increases with nitrogen doping. All ESR parameters and the response to random stress are found to be similar for the KUL2 and W15 ($[N_S–V]^-$) ESR centres. Hence, it was proposed that the centres have a common core, namely a negative vacancy (Iakoubovskii and Stesmans 2001). In contrast with that for W15, the half-field KUL2 spectrum (not shown in figure 3) exhibits not a triplet, but a doublet hf structure, suggesting that hydrogen, instead of nitrogen as in the case of W15, may be involved in the corresponding defect. This suggestion also complies with the annealing behaviour of the KUL2 centre: like the H1 centre (H–V complex), the KUL2 centre disappears upon annealing at 1400 °C for 2 h. Additional hf structure ascribed to a pair of equivalent ^{13}C atoms has been detected in the KUL2 spectrum. The KUL2 centre was attributed to a nearest-neighbour pair of $[H–V]^0$ and V^-, i.e., the $[H–2V]^-$ centre of C_{1h} symmetry. The $[H–2V]^0$ charge state has also been detected recently in LESR work (Iakoubovskii and Stesmans 2001, 2002), appearing as an $S = 1/2$ centre, with a resolved hydrogen hf structure (one H site). For the CVD films grown at $T < 1300$ °C the KUL2 signals are 5–10 times stronger than the W15 lines (see figure 3). The typical concentration of the KUL2 centre is in the 0.1–1 ppm range, but can reach 10 ppm in poor-quality films grown at fast rates. This centre was also detected in HPHT powders grown by the spontaneous synthesis method (Iakoubovskii and Stesmans 2001).

The ESR spectrum of an $S = 1/2$ ESR centre, termed KUL3, shows hf interaction with one H site with small, but rather anisotropic values of the hf matrix $\mathbf{A}_H$. The principal values of the latter could not be determined because of the peculiarity of powder pattern ESR spectra: in most cases they provide not the principal, but diagonal components of the **A**- and **D**-matrices in an axis system where the **g**-matrix is diagonal. The diagonal components of the hydrogen hf matrix for the KUL3 centre have been measured as $A_{1H} = 0.10$ mT, $A_{2H} < 0.02$ mT, $A_{3H} = 0.26$ mT; here, and further on in the text, the A_1-direction is chosen along the defect

Table 3. The line spectral position (in cm^{-1}) measured at 300 K for the hydrogen-related optical absorption centres in CVD samples, 100% enriched in the isotopes from the first column (Fuchs *et al* 1995). The accuracy is ~0.5 cm^{-1}.

^{12}C:^{1}H	3123.6	3323	5572	6870	7238	7366
^{13}C:^{1}H	3114.5	3317	5572	6872	7240	7378
^{12}C:^{2}H	*	*	5549	6833	7191	7324

* The peak has disappeared.

axis. This centre could only be detected in nitrogen-free CVD diamond with N_S^0 concentration below 0.1 ppm. It anneals out at 1400 °C giving rise to a very similar $S = 1/2$ spectrum, labelled KUL4. Like the KUL3 centre, the KUL4 centre exhibits a small and anisotropic hydrogen hf matrix (one H site), but the anisotropy is smaller for the latter (diagonal values $A_{1H} = 0.105$ mT, $A_{2H} = 0.087$ mT, $A_{3H} = 0.112$ mT).

A characteristic feature of the KUL3, KUL4 defects, and of KUL1, a centre that will be discussed later, is a large deviation Δg of their g-factors from the free-electron g-value (2.002 319...; see table 2). The most common reason for the g-anisotropy is SO coupling. The SO coupling constant is relatively small for light atoms (C, N, etc), and, consequently, Δg is small ($<10^{-3}$) for most intrinsic and nitrogen-related defects in diamond (Ammerlaan 1989, Newton 1994). However, for heavy elements with a large SO constant (Ni, Co, etc), in diamond, Δg can be of the order of g itself. The relatively large Δg for the KUL1, 3, and 4 ESR centres possibly indicates that they involve an as-yet unidentified impurity with a medium SO coupling strength (e.g., Si or O).

Six hydrogen-related optical absorption centres have been discovered by absorption measurements on CVD films grown from ^{13}C- and ^{2}H-enriched gases (see table 3). Peaks at 3123.6 and 3323 cm^{-1} (positions for diamond with normal isotopic content) originate from vibronic absorption, while lines at 5572, 6870, 7238, and 7366 cm^{-1} are ZPLs of electronic transitions. The corresponding defects show substantial strength in absorption and therefore should be present in concentrations above 1 ppm. No change in the position of the above-mentioned lines was observed upon making the substitution $^{14}N \rightarrow {}^{15}N$, suggesting that nitrogen is not involved in those centres. They are observed both in nitrogen-doped and nitrogen-free samples and therefore, are probably irrelevant to the KUL3 and KUL4 ESR centres, which, as mentioned before, are restricted to nitrogen-free films. As evidenced by the optical absorption data, the temperature stability of the 7366 cm^{-1} centre (0.913 eV, peak 2 in figure 2) is amazing. While all hitherto known hydrogen-related defects in CVD diamond show strong changes upon annealing in the temperature range 1300–1500 °C, the intensity of the 7366 cm^{-1} peak remains almost constant versus the CVD growth temperature in the range 1300–2100 °C (Iakoubovskii *et al* 2000c).

Using SIMS (Chevallier *et al* 1998) and capacitance–voltage (Zeisel *et al* 1999b) measurements on B-doped samples treated in a deuterium plasma, it has been demonstrated that deuterium, and consequently hydrogen, can passivate boron acceptors in CVD diamond. However, no IR absorption signature has been found yet for the boron–deuterium pairs presumably produced.

5.4.2. Lithium. The only solid evidence of Li incorporation in CVD diamond was obtained from SIMS studies (Nijenhuis *et al* 1997, Nesladek *et al* 1996). However, the measured SIMS profiles showed a rapidly decaying shape typical for the recoil mechanism discussed in section 3.4 and, therefore, can hardly be considered as evidence for Li doping. Meanwhile, no significant effect of Li doping on luminescence (Popovici *et al* 1995c, 1997), photocurrent

(Zeisel *et al* 2000), or on absorption spectra (Nesladek *et al* 1996) has been observed yet. So, the question of whether or not Li may be incorporated in diamond remains open.

5.4.3. Boron. The efficiency of incorporation of boron into CVD diamond, defined as the B/C ratio in the film divided by the B/C ratio in the feed gas, is close to unity. Therefore, boron concentrations in CVD films as high as 1% can be achieved (e.g., Eccles *et al* (1999)). Boron is preferentially incorporated as a substitutional acceptor, thus constituting the dominant defect in boron-doped CVD diamond. CVD films containing uncompensated nitrogen donors show an absorption feature (see No 8 in figure 1), which can be interpreted as a broad peak centred at 4.6 eV, tentatively attributed to the $[B_S–N_S]^0$ pair (see section 4.2.2). Alternatively, the 4.6 eV peak in CVD diamond had also tentatively been ascribed to the absorption transitions between the π-bands in graphite inclusions (Khomich *et al* 2000). Boron-related broad luminescence bands at 2.3 and 4.6 eV, which are frequently observed in CVD diamond, have been described in section 4.3.

5.4.4. Nitrogen. Ion channelling results reveal that like boron, nitrogen mostly incorporates in CVD diamond as a single atom, into the substitutional site (Samlenski *et al* 1996). However, typically reported (Eccles *et al* 1999, Leeds *et al* 1999) incorporation efficiencies for nitrogen (10^{-4}–10^{-3}) are much lower than that for boron ($\sim$1). The explanation for this result came from *in situ* mass spectroscopical studies (Leeds *et al* 1999): nitrogen in the feed gas is present mostly as N_2 molecules, either added intentionally or originating from vacuum leaks. Because of the strength of the N≡N bond, a large proportion of N_2 molecules can survive non-dissociated in the plasma in many CVD reactors. However, if weaker compounds, such as NH_3 and urea, are used for nitrogen doping, then a high nitrogen dissociation rate and, consequently, high nitrogen incorporation ratio ($\sim$1), can be achieved (Edgar *et al* 1998).

There is a common belief that due to the low deposition temperature there should be no nitrogen complexes in CVD diamond. However, some CVD films show PL lines from the $[2N_S–V]^0$ (H3) centres (Collins *et al* 1990, Lin *et al* 1996). This PL can be particularly strong in ⟨100⟩-oriented CVD films and HPHT crystals. A nitrogen pair in the $2N_S$–V centre can be formed via the aggregation of single nitrogen atoms or by direct incorporation of a N_2 molecule in combination with a vacancy. The particular dependence of the H3 PL intensity measured on the growth temperature in the temperature range 800–2100 °C rejects the first possibility, thus evidencing the possibility of molecular incorporation of nitrogen in diamond (Iakoubovskii *et al* 2000c). However, the concentration ratio of the $[2N_S–V]^0$ to the N_S^0 centres was estimated to be less than 10^{-3}, indicating a low efficiency of such molecular incorporation.

The dominant nitrogen centre in CVD diamond is N_S. Combination of SIMS and ESR revealed that at relatively low nitrogen doping levels ($<$ 50 ppm in the film) most of the nitrogen in CVD films is present in the N_S^0 form. However, no significant increase in the N_S^0 content is observed at higher doping level. It was suggested that at high doping level the a-C-related defects, whose concentration usually increases with nitrogen doping, push the Fermi level position down from the level $E_C - 1.7$ eV, in lightly doped film, towards $E_V + 1$ eV, in highly doped samples, thus converting N_S^0 to the N_S^+ charge state (Iakoubovskii and Adriaenssens 2000e).

The fact of compensation of defects in CVD diamond is further confirmed by PL measurements on the N_S–V centres, which are commonly detected in CVD and HPHT diamond. While the 1.945 eV line, originating from the $[N_S–V]^-$ charge state, is exclusively detected in HPHT diamond, both the 1.945 eV ($[N_S–V]^-$) and 2.156 eV (assumed to be $[N_S–V]^0$) systems are observed in CVD films. A typical concentration of the $[N_S–V]^-$ complexes

in CVD diamond has been inferred by means of ESR as ∼0.1 ppm (Iakoubovskii and Stesmans 2001). This low value is in agreement with the non-detection of the 1.945 and 2.156 eV lines in optical absorption studies (Iakoubovskii *et al* 2000c).

A previously undocumented nitrogen-related centre, termed KUL5, has been detected recently by means of ESR (Iakoubovskii and Stesmans 2001). Fitting of the spectra revealed that it relates to an $S = 1/2$ centre, characterized by an isotropic g-factor of 2.002 91 and isotropic nitrogen hf matrix with diagonal components of 0.074 mT. The isotropy of the **A**-matrix was confirmed by measurements on single-grain CVD samples. It may suggest that nitrogen is distant from the unpaired spin.

5.4.5. Oxygen. Because of the unfortunate natural isotopic composition (99.762% of ^{16}O ($I = 0$) and only 0.038% of ^{17}O ($I = 5/2$) and 0.2% of ^{18}O ($I = 0$)), detection of oxygen in diamond by ESR or by isotopic substitution analysis of optical spectra is difficult, and has not been reported yet. By comparing CL spectra from CVD films grown under similar conditions, with and without O_2 gas added into the microwave CVD reactor, CL lines at 2.725, 2.702, 2.696, 2.692, 2.681, 2.676 eV have been ascribed to oxygen-related optical centres (Ruan *et al* 1993).

5.4.6. Sulphur. First reports on successful doping of CVD diamond by introducing H_2S gas into a microwave CVD reactor (Sakaguchi *et al* 1999) or by S^+ implantation (Hasegawa *et al* 1999) were strongly doubted by Kalish *et al* (2000), who have shown that the observed conductivity in the samples used by Sakaguchi *et al* was caused not by n-type sulphur doping but by p-type boron contamination. The former group (Sakaguchi *et al* 1999) has recently again reported on successful n-type doping of CVD diamond by sulphur (Nishitani-Gamo *et al* 2001), but these results need to be confirmed. Possibly sulphur can form a substitutional double donor in diamond, but it may be compensated by B_S or a-C-related acceptors. Recently, a p–n junction was manufactured using S-doped CVD diamond film grown on a B-doped HPHT crystal (Horiuchi *et al* 2001). By utilizing the p–n junction properties, efficient electroluminescence has been obtained.

5.4.7. Silicon. As mentioned in section 5.1, there are two main sources of Si in CVD diamond: diffusion of Si atoms out of the Si substrate into the CVD film and incorporation of Si ions etched off the fused silica windows by the plasma. Combination of SIMS and PL techniques revealed that the first contribution produces an intense peak in the Si-atom distribution at the Si–diamond interface, while the second contribution creates a uniform, though relatively weak profile, across the film thickness (Dollinger *et al* 1995, Weima *et al* 2000).

The 1.682 eV Si-related line (No 4 in figure 2) was used in spatial PL monitoring of Si by Dollinger *et al*. This line, which is seen in almost all CVD diamond films, was thoroughly characterized by means of absorption, PL, and CL. Measurements on homoepitaxial films with the lowest stress allowed twelve peaks to be resolved, forming three groups of four lines, within the 1.682 eV ZPL. The appearance of those three groups is accepted as originating from the three isotopes of Si (natural abundances of 92.23% (^{28}Si, $I = 0$), 4.67% (^{29}Si, $I = 1/2$), and 3.1% (^{30}Si, $I = 0$)). However, the intensity of those lines was interpreted as resulting either from one (Clark *et al* 1995) or from two (Zaitsev 2001) Si sites. The latter interpretation agrees with the observed quadratic dependence of the 1.682 eV PL intensity on the Si^+ implantation dose (Zaitsev 2001). Temperature-resolved PL and absorption measurements revealed that the four lines within each of the three groups originate from transitions between the ground state split by 0.2 meV and the excited state split by 1.07 meV for the same defect (Clark *et al* 1995).

The intensity of the 1.682 eV system slowly increases with annealing temperature in the range 1000–2200 °C (Clark and Dickerson 1991, Ruan *et al* 1991).

PLE measurements on the 1.682 eV line reveal an oscillatory spectrum from which a ground-state level at $E_C - 2.05$ eV was deduced. This conclusion was further corroborated by observation of an absorption threshold at 2 eV (label 7 in figure 2), whose appearance correlated with the presence of the 1.682 eV line in the absorption spectrum (Iakoubovskii and Adriaenssens 2000e). The $E_C - 2.05$ eV position of the ground state puts the excited state of the 1.682 eV centre close to the diamond conduction band, making possible photothermal ionization processes. The latter could account for a previous unusual observation in that the integrated absorption intensity of the 1.682 eV system decreases with increasing temperature, while it is constant for all other known centres in diamond (Collins *et al* 1994). The 1.682 eV centre shows a very weak vibronic structure both in luminescence and absorption, with no mirror symmetry relative to the ZPL. The intensity of the 1.682 eV absorption line can be increased up to ten times by UV illumination, reaching a level of 25% of absorption. This result shows that another charge state of the defect more positive than that responsible for the 1.682 eV line is dominant in CVD diamond. However, no narrow-line absorption, which could be ascribed to that state, could be traced in the range 0.5–5.5 eV (see, e.g., figure 1). The 1.682 eV line in polycrystalline CVD diamond is often accompanied by a broader underlying peak at 1.679 eV. Combined absorption and PL measurements reveal that the latter is not an independent ZPL, but probably a stress-induced feature related to the 1.682 eV centre, which can be removed by annealing for 2 h at 1400 °C (Iakoubovskii *et al* 2001).

No justified model for the 1.682 eV centre has been proposed yet. In irradiated CVD diamond the intensity of the 1.682 eV absorption line increases as vacancies anneal out. Therefore, it was concluded that the corresponding defect involves a vacancy, and a Si_S–V model had been proposed (Collins *et al* 1994). Subsequent calculations show that the Si_S–V structure is unstable: the Si atom relaxes towards the centre of a divacancy forming a VSiV centre of trigonal symmetry (Goss *et al* 1996). However, polarization-resolved PL measurements reveal not a C_3, but a C_2 symmetry axis for the 1.682 eV centre (Brown and Rand 1995). Clearly, ESR and ODMR measurements will have to be involved in order to clarify the structure of the corresponding defect. A first step in this direction was made by Sternschulte *et al* (1995), who have measured the Zeeman splitting of the 1.682 eV PL and absorption lines. The splitting pattern is complex and it has not been successfully interpreted.

The 1.682 eV line is often accompanied by a weaker absorption peak at 1.640 eV (peak 3 in figure 2). When the intensity of the 1.682 eV peak is observed to increase with UV illumination, then the intensity of the 1.640 eV line remains almost unchanged, which would suggest that those lines originate from different centres (Iakoubovskii and Adriaenssens 2000e). Yet, polishing away a few microns on the substrate side of a 200 μm thick CVD sample results in the disappearance of both 1.682 and 1.640 eV absorption lines, hinting that both centres are Si related.

The KUL1 ESR spectrum (see figure 3) was originally assigned to the $[VNiV]^0$ defect, involving a neutral Ni atom at the centre of a divacancy (Iakoubovskii *et al* 2000b). However, later measurements revealed additional hf structure, which appeared inconsistent with this model (Iakoubovskii and Stesmans 2001). The following parameters were extracted from fitting the updated ESR spectrum: $S = 1$, $g_1 = 2.0041(1)$, $g_2 = g_3 = 2.0035$ (previously: $g_1 = g_2 = g_3 = 2.0039$), $D = 35.8$ mT (300 K), $E < 0.01$ mT. The value of D was observed to decrease linearly with decreasing temperature. Three sets of hf lines were detected. Two sets probably originate from hf interaction with one and two equivalent carbon sites (^{13}C). The third could be attributed to four equivalent carbon sites or to one Si site (^{29}Si). Polishing away a thin layer on the substrate side of a CVD film results in the disappearance of the KUL1

spectrum, while no change is observed in the intensity of the P1, W15, KUL2, 5, and 6 ESR signals. This result indicates that a Si atom is involved in the structure of the KUL1 centre, but the KUL2, 5, and 6 centres are not Si related. This leaves the atomic structure of the KUL1 defect undecided.

5.4.8. Phosphorus. Currently, only a few research groups have succeeded in achieving reliable and reproducible introduction of phosphorus into homoepitaxial CVD diamond. The phosphorus content can reach 50 ppm in the ⟨111⟩-oriented films, but doping of layers of other orientations has not been achieved yet (Koizumi 1999). From their SIMS data, the phosphorus incorporation efficiency can be inferred as ∼0.02. Recent RBS measurements reveal that more than 90% of those phosphorus atoms occupy substitutional lattice sites (Hasegawa *et al* 2001). Hall measurements on phosphorus-doped films demonstrate n-type conductivity with an activation energy of 0.55 eV (Koizumi 1999). CL spectra from those samples show sharp UV peaks ascribed to DA pair recombination with substitutional phosphorus (P_S) as the donor and B_S as the acceptor (Sternschulte *et al* 1999). Fitting of CL spectra with the DA model yields a ground-state position for P_S as $E_C - 0.63$ eV, which is close to the activation energy obtained from Hall measurements. More reliable determination of the P_S energy levels was performed using a combination of absorption and photothermal ionization (Haenen *et al* 2000, Gheeraert *et al* 1999, 2000) spectroscopies. The position of the P_S ground state was deduced as $E_C - 0.60$ eV and four excited states have been detected at 0.523, 0.565, 0.575, and 0.584 V above the ground state.

Several ESR studies of P-implanted CVD and HPHT diamonds have been reported (Isoya *et al* 1997b, Zvanut *et al* 1994, Casanova *et al* 2001). In these works, an observed isotropic doublet signal with $g = 2.0024$ and $A \sim 2.8$ mT is attributed to a P_S^0 donor centre. However, before successful and reliable assignment can be concluded, several points need to be further clarified:

(1) The presence of a strong line at the centre of the doublet in all reported P-related ESR spectra may raise doubts as to the assignment of the doublet to an $I = 1/2$ impurity with 100% abundance.
(2) The variation over the previous works in the reported hf values is unacceptably large for a unique defect centre.
(3) Moreover, results on ion-implanted samples should always be treated with some caution, as, unavoidably, every implanted ion produces numerous irradiation-related defects. As a consequence, the corresponding ESR spectra are rich in lines and hence the spectrum is difficult to interpret (Loubser and van Wyk 1978).

No ESR results on CVD films doped with phosphorus during their growth have been published so far. A possible reason for this may be that the synthesis of phosphorus-doped CVD samples is mostly performed on Ib-type nitrogen-rich diamond substrates, which give strong background N_S^0 signals. Obviously, films grown on IIa samples are required for adequate ESR studies.

5.4.9. Metal-related centres. It had been thought that metal evaporation from the spiral, used in hot-filament CVD, leads to incorporation of W, Ta, or Re into CVD diamond and, indeed, those elements were detected in CVD films by NAA (Menon *et al* 1999). More unexpected was the observation of Mo and stainless steel metals (probably Ni, Cr, and Fe) at the 1% level by means of Rutherford backscattering in CVD films grown by microwave-assisted CVD (Iakoubovskii *et al* 2000b). And perhaps even less expected was the fact that some of these

large atoms, in particular W, and possibly Ta and Ni, appear to form defect centres in CVD diamond.

PL and CL lines at 1.735, 1.741, 1.75, 1.754, 1.759, and 1.774 eV have been associated with W and Ta impurities, respectively, in CVD diamond (Zaitsev 2000). In poor-quality samples (excessive non-diamond carbon inclusions), an unresolved combination of those lines together with their vibronic structure forms a broad band centred at ∼1.7 eV. The assignment is based on the correlation of the appearance of those lines with the use of the spiral made of the corresponding metal in hot-filament CVD. The interpretation is further supported by the analysis of the vibronic structure, which reveals very weak vibronic coupling and low vibronic energy (∼25 meV), indicating the presence of a heavy impurity in all those centres (Zaitsev 2000).

An unusual PL system has been characterized recently in nitrogen-free CVD diamond grown by microwave-assisted CVD (Iakoubovskii *et al* 2000b). It consists of five groups of three 9 meV split lines centred at 2.20, 2.10, 2.02, 1.92, and 1.83 eV. The triplet structure could only be resolved at low temperatures (<150 K) in samples with small residual stress. No temperature dependence of the relative intensities of the triplet lines was observed. Their ratio (∼18:6:1) is close to the natural abundance of the main Ni isotopes (68.27% ^{58}Ni, 26.1% ^{60}Ni, and 3.59% ^{62}Ni), and therefore, it was concluded that one Ni atom is part of the corresponding defect. PLE measurements revealed an oscillatory structure, from which the ground-state level of the corresponding defect was inferred as $E_C - 2.24$ eV. It was suggested that the above-mentioned five series of lines originate from the electronic transitions between a common ground state and a series of excited states.

The 15-line PL spectrum increased about 1.5 times upon annealing at 1000 °C for 2 h and about 3 times upon annealing at 1400 °C for 2 h. The same behaviour was observed for the KUL1 ESR centre. The intensities of the KUL1 spectrum and of the PL lines appear to correlate linearly in different samples (Iakoubovskii *et al* 2000b); however, later measurements on a larger set of CVD samples suggest this correlation to have been fortuitous, rather than reflecting a real feature.

Two more triplets of PL lines observed in as-grown CVD films may possibly originate from a defect involving a heavy impurity. The first system consists of 18 meV spaced lines at 1.775, 1.793, and 1.811 eV (Berthou *et al* 1999) and the second involves peaks at 1.586, 1.575, and 1.568 eV (Zaitsev 1998, figure 67).

5.4.10. Optical centres of unknown nature in CVD diamond. A series of absorption lines at 1.310, 1.423, 1.446, and 1.496 eV in CVD diamond have been reported by Allers and Collins (1995). PC spectra measured on the same samples exposed a threshold at 1.5 eV with superimposed oscillatory structure. This threshold was assigned to a defect with ground state at $E_C - 1.5$ eV.

Many PL and CL spectra from CVD diamond films show ZPLs at 2.33, 2.42, 2.48, 2.537, 2.547, 2.557, 2.567, 2.572, and 2.99 eV (Ruan *et al* 1991, 1993, Collins *et al* 1990, Partlow *et al* 1990) characterized by a relaxation time of 0.0096, not determined, 1.0, 1.8, 1.3, 1.2, 1.5, 1.3, and 0.063 μs, respectively (Khong *et al* 1994). The temperature dependences of the intensities of the 2.33, 2.48, and 2.567 eV CL peaks have been documented by Khong and Collins (1993). Careful analysis of the vibronic structure suggests that the 2.99 eV line is not related (Khong *et al* 1994) to the $[3N_S–V]^0$ defect (N3 optical centre, ZPL at 2.985 eV), which is typically observed in Ia diamond. The intensities of the 2.42 and 2.567 eV lines, but not of the others, correlated linearly over different samples (Khong and Collins 1993). The 2.33 eV peak is often split into a doublet (Ruan *et al* 1991). The splitting distance can vary spatially, even within one sample, and, therefore, it is probably strain induced. This 2.33 eV feature is stable against annealing for 2 h at 1350 °C (Ruan *et al* 1991).

Collins *et al* (1989) listed extra luminescence lines at 2.200, 2.466, 2.497, 2.599, 2.67, 2.756, 2.786, 3.092, 3.272 as unique for CVD diamond. A series of CL lines at 2.07, 2.11, 2.20, 2.24, 2.28, 2.33, 2.37, 2.41, 2.46, 2.5, 2.57, 2.62, and 2.67 eV were fitted with the DA recombination model (Dischler *et al* 1994). However, the inconstancy of the relative intensities of these lines over different samples noticed by authors raises doubts about this interpretation. Many PL spectra from CVD films together with the $[N_S–V]^-$ line at 1.945 show a ZPL at 1.967 eV (e.g., Ruan *et al* 1991). Unlike the former, the latter line can be excited in CL. The 1.967 eV line is stable against annealing in the range 1000–2200 °C (Zaitsev 1998).

5.4.11. ESR centres of unknown nature in CVD diamond. Annealing of CVD diamond at 1600 °C for 4 h can produce an $S = 1/2$ ESR centre with $g = 2.0035$ (Talbot-Ponsonby *et al* 1998). Another $S = 1/2$ centre with $g_1 = 2.003\,07$, $g_2 = g_3 = 2.002\,92$, labelled as KUL6, was reported in as-grown CVD films (Iakoubovskii and Stesmans (2001); see figure 4). The centre disappears upon annealing at 1400 °C for 2 h and shows no detectable allowed or forbidden hf structure.

6. Concluding remarks

6.1. What we have learned so far from studying defects in CVD diamond

Although CVD diamond material exhibits a rather unfortunate morphology—most films are heavily strained, inhomogeneous, randomly oriented polycrystalline layers—the study of the defects in this 'young' material has already contributed to the general knowledge of defects in solids. For example, the characterization of the H–V ESR centre in CVD diamond has helped to identify the H–V defect in silicon (Watkins 2001). Some results on the broad-band luminescence obtained for CVD diamond have improved the understanding of this—for all types of diamond—common phenomenon (see section 4.3). Finally, the possibility of incorporation of molecular nitrogen into the growing diamond film was revealed by studying the $[2N_S–V]^0$ centre in CVD films (see section 5.4.4). It was shown that an easy monitoring of effects of random stress on optical and ESR centres in diamond could be realized by using a series of properly selected CVD samples (Iakoubovskii *et al* 1999, Iakoubovskii and Stesmans 2001).

6.2. Trends and proposals for further study of defects in CVD diamond

- Currently, much research is carried out aiming to reduce the temperature of CVD growth in order to make CVD diamond compatible with the microelectronics technology. Growth temperatures as low as 150 °C have been reported (e.g., Hiraki (2000)). At temperatures below 600 °C (350 °C) vacancies (interstitials) should be immobile in diamond and they can be present in CVD films grown at low temperatures. It is worth noting that in low-temperature CVD diamond, vacancies and interstitials are produced *during* the growth instead of being created by post-growth irradiation. Consequently, ESR and optical study of this material may provide new information on the properties of primary intrinsic defects in diamond.
- It is believed that in the near future, control over n-type doping of CVD diamond by sulphur and phosphorus will be achieved, and S- and P-doped samples will become widely available. This can open new areas in the study of defects in CVD diamond: sulphur- and phosphorus-related centres can be characterized by ESR, PL, IR absorption and other techniques (e.g., ion channelling will be beneficial). In n-type CVD diamond it will be

possible to raise the Fermi level to closer to the conduction band and thus possibly uncover some more defects which could have been missed because of their inappropriate charge (spin) state.

- Thanks to ESR and optical work carried out by the King's College London and Oxford diamond groups, the transformation of vacancies and interstitials in diamond (both single crystals and CVD diamond) upon annealing up to about 900 °C is largely understood. This work should be continued towards higher temperatures, aiming at characterization of multivacancy, multi-interstitial, and mixed defects. These defects have special importance for CVD diamond, where, owing to the relatively high growth temperature, the vacancies and interstitials should occur in aggregated forms.
- In the past systematic research has been performed on the incorporation of a wide range of elements by introducing them into HPHT diamonds during their growth (General Electric, NIRIM, former Soviet Union, etc) and by post-growth ion implantation (the groups of Vavilov (Moscow), Kalish (Haifa), and Prins (Pretoria)). Although the main objective was to search for new dopants and HPHT catalysts for technical applications, this research produced many interesting scientific results. In particular, it was demonstrated that even such large atoms as Ne, Ti, Cr, Co, Ni, Zn, As, Zr, Ag, Xe, and Tl can form defect centres in diamond (Zaitsev 1998, 2000, 2001). The examples of W and Ta show that impurity incorporation during the growth can be favoured in CVD diamond. As it may be easy to achieve incorporation of a wide range of elements in this material just by introducing a solid or gaseous dopant into the plasma, this study could prove beneficial, both for physics and technology, by discovering new dopants and colour centres in diamond.
- Only six hydrogen-related (see table 3), nine nitrogen-related (N_S^0, N_S^-, KUL5, $[2N_S{-}V]^0$, $[N_S{-}V]^-$, and the optical centres 2.156, 2.086, 2.807, and 3.188 eV), and perhaps six oxygen-related centres (see section 5.4.5) have thus far been detected in CVD diamond. Meanwhile, there are many PL lines of unknown origin, which are specific to CVD films. It is likely that (combined) PL and ESR studies of samples enriched in ^{2}H, ^{17}O, and ^{15}N will directly aid the identification of many hydrogen-, nitrogen-, and oxygen-related centres in CVD diamond, and many more exciting results as regards atomic identification may be expected there.
- It is possible that in order to reveal impurity-related optical and ESR centres in CVD diamond, irradiation and annealing may be required. In the few such studies reported so far, no new PL and ESR centres have been observed. However, this work should be extended to a wider range of samples and characterization techniques.

References

Alekseev A G, Amosov V N, Krasil'nikov A V, Tugarinov S N, Frunze V V and Tsutskikh A Y 2000 *Tech. Phys. Lett.* **26** 496

Allers L and Collins A T 1995 *J. Appl. Phys.* **77** 3879

Allers L and Mainwood A 1998 *Diamond Relat. Mater.* **7** 261

Allers L, Collins A T and Hiscock J 1998 *Diamond Relat. Mater.* **7** 228

Ammerlaan C A J 1989 *Landolt–Börnstein New Series* Group III, vol 22b, ed O Madelung and M Schultz (Berlin: Springer) p 177

Anastassakis E and Burstein E 1970 *Phys. Rev.* B **2** 1952

Asmussen J and Reinhard D 2001 *Diamond Films Handbook* (New York: Dekker)

Baker J M and Newton M E 1994 *Appl. Magn. Reson.* **7** 209

Baker J M and Newton M E 1995 *Appl. Magn. Reson.* **8** 207

Bell M D and Leivo W J 1967 *J. Appl. Phys.* **38** 337

Bergman L, McClure M T, Glass J T and Nemanich R J 1994 *J. Appl. Phys.* **76** 3020

Berthou H, Faure C, Hanni W and Perret A 1999 *Diamond Relat. Mater.* **8** 636

Bharuth-Ram K, Quintel H, Restle M, Ronning C, Hofsass H and Jahn S G 1995 *J. Appl. Phys.* **78** 5180
Bharuth-Ram K, Burchard A, Deicher M, Quintel H, Restle M, Hofsass H and Ronning C 2001 *Phys. Rev.* B **64** 195207
Braunstein G and Kalish R 1981 *Appl. Phys. Lett.* **38** 416
Brown S W and Rand S C 1995 *J. Appl. Phys.* **78** 4069
Casanova N, Gheeraert E, Deneuville A, Uzan-Saguy C and Kalish R 2001 *Diamond Relat. Mater.* **10** 580
Chevallier J, Theys B, Lusson A and Grattepain C 1998 *Phys. Rev.* B **58** 7966
Clark C D, Ditchburn R W and Dyer H B 1956 *Proc. R. Soc.* A **237** 75
Clark C D and Dickerson C B 1991 *Surf. Coatings Technol.* **47** 336
Clark C D, Kanda H, Kiflawi I and Sittas G 1995 *Phys. Rev.* B **51** 16 681
Collins A T 1979 *Defects and Radiation Effects in Semiconductors Inst. Phys. Conf. Ser. 46* (Bristol: Institute of Physics Publishing) p 327
Collins A T and Rafique S 1979 *Proc. R. Soc.* A **367** 81
Collins A T and Spear P M 1986 *J. Phys. C: Solid State Phys.* **19** 6845
Collins A T, Szechi J and Tavender S 1988a *J. Phys. C: Solid State Phys.* **21** L161
Collins A T, Davies G, Kanda H and Woods G S 1988b *J. Phys. C: Solid State Phys.* **21** 1363
Collins A T and Lawson S C 1989 *J. Phys.: Condens. Matter* **1** 6929
Collins A T, Kamo M and Sato Y 1989 *J. Phys. D: Appl. Phys.* **22** 1402
Collins A T, Kamo M and Sato Y 1990 *J. Mater. Res.* **5** 2507
Collins A T 1992 *Diamond Relat. Mater.* **1** 457
Collins A T 1993 *Physica* B **185** 284
Collins A T, Allers L, Wort C J H and Scarsbrook G A 1994 *Diamond Relat. Mater.* **3** 932
Collins A T 1999 *Diamond Relat. Mater.* **8** 1455
Collins A T 2000 *Diamond Relat. Mater.* **9** 417
Correia J G, Marques J G, Alves E, Forkel-Wirth D, Jahn S G, Restle M, Dalmer M, Hofsass H and Bharuth-Ram K 1997 *Nucl. Instrum. Methods* B **127–8** 723
Cytermann C, Brener R and Kalish R 1994 *Diamond Relat. Mater.* **3** 667
Davies G 1974 *J. Phys. C: Solid State Phys.* **7** 3797
Davies G and Hammer M F 1976 *Proc. R. Soc.* A **348** 285
Davies G, Nazaré M H and Hammer M F 1976 *Proc. R. Soc.* A **351** 245
Davies G 1979 *J. Phys. C: Solid State Phys.* **12** 2551
Davies G and Nazaré M H 1980 *J. Phys. C: Solid State Phys.* **13** 4127
Davies G 1981 *Rep. Prog. Phys.* **44** 787
Davies G, Foy C and O'Donnel K 1981 *J. Phys. C: Solid State Phys.* **14** 4153
Davies G, Collins A T and Spear P 1983 *Solid State Commun.* **49** 433
Davies G, Lawson S C, Collins A T, Mainwood A and Sharp S J 1992 *Phys. Rev.* B **46** 13 157
Davies G 1999 *Physica* B **273+4** 15
Davies G, Smith H and Kanda H 2000 *Phys. Rev.* B **62** 1528
Dean P J 1965 *Phys. Rev.* **139** A588
Dischler B, Rothemund W, Wild C, Locher R, Biebl H and Koidl P 1994 *Phys. Rev.* B **49** 1685
Dischler B (ed) 1998 *Low-Pressure Synthetic Diamond: Manufacturing and Applications* (Heidelberg: Springer)
Dollinger G, Bergmaier A, Frey C M, Roesler M and Verhoeven H 1995 *Diamond Relat. Mater.* **4** 591
Doyle B P, Storbeck E J, Wahl U, Connell S H and Sellschop J P F 2000 *J. Phys.: Condens. Matter* **12** 67
Eccles A J, Steele T A, Afzal A, Rego C A, Ahmed W, May P W and Leeds S M 1999 *Thin Solid Films* **343+4** 627
Edgar J H, Xie Z Y and Braski D N 1998 *Diamond Relat. Mater.* **7** 35
Evans T and Qi Z 1982 *Proc. R. Soc.* A **381** 159
Fizgeer B, Uzan-Saguy C, Cytermann C, Richter V, Avigal I, Shaanan M, Brener R and Kalish R 2001 *Phys. Status Solidi* a **186** 281
Fuchs F, Wild C, Schwarz and Koidl P 1995 *Diamond Relat. Mater.* **4** 652
Fujita T, Abd-Elrahman M I, Takiyama K and Oda T 1996 *Phil. Mag.* B **74** 359
Gippius A A, Vavilov V S, Zaitsev A M and Zhakupbekov B S 1983 *Physica* B **116** 187
Gippius A A 1993 *Diamond Relat. Mater.* **2** 640
Gheeraert E, Koizumi S, Teraji T, Kanda H and Nesladek M 1999 *Phys. Status Solidi* a **174** 39
Gheeraert E, Koizumi S, Teraji T and Kanda H 2000 *Solid State Commun.* **113** 577
Gonon P, Deneuville A, Gheeraert E and Fontaine F 1994 *Diamond Relat. Mater.* **3** 836
Gonon P, Deneuville A, Fontaine F and Gheeraert E 1995 *J. Appl. Phys.* **78** 6633
Gorbatkin S M, Zuhr R A, Roth J and Naramoto H 1991 *J. Appl. Phys.* **70** 2986
Goss J P, Jones R, Breuer S J, Briddon P R and Oberg S 1996 *Phys. Rev. Lett.* **77** 3041

Gruber A, Drabenstedt A, Tietz C, Fleury L, Wrachtrup J and von Borczyskowski C 1997 *Science* **276** 2012
Haenen K, Meykens K, Nesladek M, Knuyt G, Stals L M, Teraji T and Koizumi S 2000 *Phys. Status Solidi* a **181** 11
Hanzawa H, Nishikori H, Nisida Y, Sato S, Nakashima T, Sasaki S and Miura N 1993 *Physica* B **184** 137
Haque M S, Naseem H A, Shultz J L, Brown W D, Lal S and Gangopadhyay S 1998 *J. Appl. Phys.* **83** 4421
Hasegawa M, Takeuchi D, Yamanaka S, Ogura M, Watanabe H, Kobayashi N, Okushi N and Kajimura K 1999 *Japan. J. Appl. Phys.* **38** L1519
Hasegawa M, Teraji T and Koizumi S 2001 *Appl. Phys. Lett.* **79** 3068
Hayashi K, Watanabe H, Yamanaka S, Okushi H and Kajimura K 1996 *Appl. Phys. Lett.* **69** 1122
He Xing-Fei, Fisk P T H and Manson N B 1992 *J. Appl. Phys.* **72** 211
He Xing-Fei, Manson N B and Fisk P T H 1993a *Phys. Rev.* B **47** 8809
He Xing-Fei, Manson N B and Fisk P T H 1993b *Phys. Rev.* B **47** 8816
Hiraki A 2000 *Appl. Surf. Sci.* **162–3** 326
Hiromitsu I, Wesra J and Glasbeek M 1992 *Phys. Rev.* B **46** 10 600
Horiuchi K, Kawamura A, Ide T, Ishikura T, Nakamura K and Yamashita S 2001 *Japan. J. Appl. Phys.* **40** L275
Hunt D C, Twitchen D J, Newton M E, Baker J M, Anthony T R and Banholzer W F 2000a *Phys. Rev.* B **61** 3863
Hunt D C, Twitchen D J, Newton M E, Baker J M, Kirui J K, van Wyk J A, Anthony T R and Banholzer W F 2000b *Phys. Rev.* B **62** 6587
Iakoubovskii K, Stesmans A, Adriaenssens G J, Provoost R, Silverans R and Raiko V 1999 *Phys. Status Solidi* a **174** 137
Iakoubovskii K 2000 *PhD Thesis* Katholieke Universiteit Leuven
Iakoubovskii K and Adriaenssens G J 2000a *Phys. Status Solidi* a **181** 59
Iakoubovskii K and Adriaenssens G J 2000b *J. Phys.: Condens. Matter* **12** L77
Iakoubovskii K and Adriaenssens G J 2000c *Phil. Mag. Lett.* **80** 441
Iakoubovskii K and Adriaenssens G J 2000d *Phys. Rev.* B **61** 10 174
Iakoubovskii K and Adriaenssens G J 2000e *Diamond Relat. Mater.* **9** 1349
Iakoubovskii K, Adriaenssens G J and Nesladek M 2000a *J. Phys.: Condens. Matter* **12** 189
Iakoubovskii K, Stesmans A, Nouwen B and Adriaenssens G J 2000b *Phys. Rev.* B **62** 16 587
Iakoubovskii K, Adriaenssens G J and Vohra Y K 2000c *J. Phys.: Condens. Matter* **12** L519
Iakoubovskii K and Adriaenssens G J 2001 *J. Phys.: Condens. Matter* **13** 6015
Iakoubovskii K, Adriaenssens G J, Dogadkin N N and Shiryaev A A 2001 *Diamond Relat. Mater.* **10** 18
Iakoubovskii K and Stesmans A 2001 *Phys. Status Solidi* a **186** 199
Iakoubovskii K and Adriaenssens G J 2002 *Diamond Relat. Mater.* **11** 125
Iakoubovskii K and Stesmans A 2002 submitted
Isoya J, Kanda H, Norris J R, Tang J and Bowman M K 1990a *Phys. Rev.* B **41** 3905
Isoya J, Kanda H and Ushida Y 1990b *Phys. Rev.* B **42** 9843
Isoya J, Kanda H, Ushida Y, Lawson S C, Yamasaki S, Itoh H and Morita Y 1992 *Phys. Rev.* B **45** 1436
Isoya J, Kanda H, Sakaguchi I, Morita Y and Oshima T 1997a *Radiat. Phys. Chem.* **50** 321
Isoya J, Kanda H, Akaishi M, Morita Y and Oshima T 1997b *Diamond Relat. Mater.* **6** 356
Ittermann B *et al* 1997 *Appl. Phys. Lett.* **71** 3658
Jubber M G and Milne D K 1996 *Phys. Status Solidi* a **154** 185
Kaizer W and Bond W C 1959 *Phys. Rev.* **115** 857
Kalish R, Reznik A, Uzan-Saguy C and Cytermann C 2000 *Appl. Phys. Lett.* **76** 757
Khomich A, Ralchenko V, Nistor L, Vlasov I and Khmelnitskiy R 2000 *Phys. Status Solidi* a **181** 37
Khong Y L and Collins A T 1993 *Diamond Relat. Mater.* **2** 1
Khong Y L, Collins A T and Allers L 1994 *Diamond Relat. Mater.* **3** 1023
Kiflawi I and Lang A 1974 *Phil. Mag.* **30** 219
Kiflawi I, Mainwood A, Kanda H and Fisher D 1996 *Phys. Rev.* B **45** 1436
Kiflawi I, Sittas G, Kanda H and Fisher D 1997 *Diamond Relat. Mater.* **6** 146
Klein P B, Crossfield M D, Freitas J A Jr and Collins A T 1995 *Phys. Rev.* **51** 9634
Koizumi S 1999 *Phys. Status Solidi* a **172** 71
Koizumi S *et al* 2001 *Science* **292** 1899
Konorova A, Sergienko V F, Tkachenko S D, Shulzhenko A A, Gontar A G and Bocheka A A 1984 *J. Superhard Mater.* **6** 1
Kweon M C, Lee S H, Kim E M, Kim Y, Yi J Y and Bark H 2001 *J. Mater. Sci. Lett.* **20** 469
Lawson S C, Kanda H, Kiyota H, Tsutsumi T and Watanabe K 1995 *J. Appl. Phys.* **77** 1729
Lawson S C, Kanda H, Watanabe K, Kiflawi I, Sato Y and Collins A T 1996 *J. Appl. Phys.* **79** 4348
Lawson S C, Fisher D, Hunt D C and Newton M E 1998 *J. Phys.: Condens. Matter* **10** 6171
Lee S-T, Lin Zh and Jiang X 1999 *Mater. Sci. Eng.* R **25** 123

Leeds S M, May P W, Ashfold M N R and Rosser K N 1999 *Diamond Relat. Mater.* **8** 226
Lettington A H and Steeds J W 1993 *Thin Film Diamond* (Dordrecht: Kluwer)
Lin L T S, Popovici G, Mori Y, Hiraki A, Prelas M A, Spitsyn B V, Khasawinah S and Sung T 1996 *Diamond Relat. Mater.* **5** 1236
Liu H and Dandy D S 1996 *Diamond Chemical Vapor Deposition: Nucleation and Early Growth Stages* (Englewood Cliffs, NJ: Noyes)
Lomer J N and Wild A M A 1973 *Radiat. Effects* **17** 37
Loubser J H N and van Wyk J A 1978 *Rep. Prog. Phys.* **41** 1201
Maier F, Riedel M, Mantel B, Ristein J and Ley L 2000 *Phys. Rev. Lett.* **85** 3472
Mainwood A, Collins A T and Woad P J 1994 *Mater. Sci. Forum* **143–7** 29
Melton C E and Giardini A A 1976 *Nature* **263** 309
Menon P M, Edwards A, Feigerle C S, Shaw R W, Coffey D W, Heatherly L, Clausing R E, Robinson L and Glasgow D C 1999 *Diamond Relat. Mater.* **8** 101
Mita Y, Nisida Y, Suito K, Onodera A and Yazu S 1990 *J. Phys.: Condens. Matter* **2** 8567
Mita Y, Ohno Y, Adachi Y, Kanehara H and Nisida Y 1993 *Diamond Relat. Mater.* **2** 768
Mita Y 1996 *Phys. Rev.* B **53** 11 360
Nadolinny V A, Yelisseyev A P, Yuryeva O P and Feygelson B N 1997 *Appl. Magn. Reson.* **12** 543
Nadolinny V A, Yelisseyev A P, Baker J M, Newton M E, Twitchen D J, Lawson S C, Yuryeva O P and Feygelson B N 1999 *J. Phys.: Condens. Matter* **11** 7357
Nazaré M H and Neves A J 1987 *J. Phys. C: Solid State Phys.* **20** 2713
Nazaré M H, Mason P W, Watkins G D and Kanda H 1995 *Phys. Rev.* B **51** 16 741
Nazaré M H and Neves A J 2001 *Properties, Growth and Applications of Diamond* (Hitchin, UK: Institution of Electrical Engineers)
Nesladek M, Meykens K, Stals L M, Quaeyhaegens C, D'Olieslaeger M, Wu T D, Vanecek M and Rosa J 1996 *Diamond Relat. Mater.* **5** 1006
Nesladek M, Stals L M, Stesmans A, Iakoubovskii K, Adriaenssens G J, Rosa J and Vanecek M 1998 *Appl. Phys. Lett.* **72** 3306
Neves A J, Pereira R, Sobolev N A, Nazaré M H, Gehlhoff, Naser A and Kanda H 2000 *Diamond Relat. Mater.* **9** 1057
Newton M E 1994 *Properties and Growth of Diamond* ed G Davies (London: INSPEC) pp 153, 166
Newton M E 2001 Personal communication
Nijenhuis J, Cao G Z, Smits P C H J, van Enckevort W J P, Gilling L J, Alkemande P F A, Nesladek M and Remes Z 1997 *Diamond Relat. Mater.* **6** 1726
Nishitani-Gamo M, Xiao C, Zhang Ya, Yasu E, Kikuchi Yu, Sakaguchi I, Suzuki T, Sato Y and Ando T 2001 *Thin Solid Films* **382** 113
Nisida Y, Mita Y, Mori K, Okuda S, Sato S, Yazu S, Nakagawa M and Okada M 1989 *Mater. Sci. Forum* **38–41** 561
Nisida Y, Yamada Y, Uchiyama S, Mita Y, Nakashima T and Sato S 1992 *Proc. 12th Int. Conf. on Defects in Insulating Materials* (Singapore: World Scientific) p 499
Pan L S and Kania D R 1995 *Diamond: Electronic Properties and Applications* (Dordrecht: Kluwer)
Partlow W D, Ruan J, Witkowski R E, Choyke W J and Knight D S 1990 *J. Appl. Phys.* **67** 7019
Pavlik Th, Noble C and Spaeth J-M 1998 *J. Phys.: Condens. Matter* **10** 9833
Pereira E, Santos L and Pereira L 1994 *Mater. Sci. Forum* **147** 57
Piekarczyk W 1999 *Cryst. Res. Technol.* **34** 553
Popovici G, Wilson R G, Sung T, Prelas M A and Khasawinah S 1995a *J. Appl. Phys.* **77** 5103
Popovici G, Wilson R G, Sung T, Prelas M A and Khasawinah S 1995b *J. Appl. Phys.* **77** 5625
Popovici G, Prelas M A, Sung T, Khasawinah S, Melnikov A A, Varichenko V S, Zaitsev A M, Denisenko A V and Fahner W R 1995c *Diamond Relat. Mater.* **4** 877
Popovici G, Melnikov A A, Varichenko V S, Sung T, Prelas M A, Wilson R G and Loyalka S K 1997 *J. Appl. Phys.* **81** 2429
Prelas M A, Popovici G and Bigelow L K 1997 *Handbook of Industrial Diamonds and Diamond Films* (New York: Dekker)
Redman D A, Brown S, Sands R H and Rand S C 1991 *Phys. Rev. Lett.* **67** 3420
Restle M, Bharuth-Ram K, Quintel H, Ronning C, Hofsass H, Jahn S G and Wahl U 1995 *Appl. Phys. Lett.* **66** 2733
Rohrer E, Graeff C F O, Janssen R, Nebel C E, Stutzmann M, Guttler H and Zachai R 1996 *Phys. Rev.* B **54** 7874
Ronning C and Hofsass H 1999 *Diamond Relat. Mater.* **8** 1623
Rossi M C, Salvatori S and Galluzzi F 1997 *Diamond Relat. Mater.* **6** 712
Ruan J, Choyke W J and Partlow W D 1991 *J. Appl. Phys.* **69** 6632
Ruan J, Kobashi K and Choyke W J 1992 *Appl. Phys. Lett.* **60** 3138
Ruan J, Choyke W J and Kobashi K 1993 *Appl. Phys. Lett.* **62** 1379

Rzepka E, Silva F, Lusson A, Riviere A and Gicquel A 2001 *Diamond Relat. Mater.* **10** 542
Sakaguchi I, Nishitani-Gamo M, Kikuchi Yu, Yasu E, Haneda H, Suzuki T and Ando T 1999 *Phys. Rev.* B **60** R2139
Samlenski R, Haug C, Brenn R, Wild C, Locher R and Koidl P 1996 *Diamond Relat. Mater.* **5** 947
Samsonenko N D, Timchenko V I, Litvin Yu A and Bokii G B 1978 *Sov. Phys. Dokl.* **23** 762
Shaanan M and Kalish R 2000 *Nucl. Instrum. Methods* B **171** 332
Sharda T, Rahaman M M, Nukaya Y, Soga T, Jimbo T and Umeno M 2001 *Diamond Relat. Mater.* **10** 561
Smith W V, Sorokin P P, Gelles I L and Lasher G J 1959 *Phys. Rev.* **115** 1546
Soper S, Nutter H L, Keller R, Davis L M and Shera E B 1993 *Photochem. Photobiol.* **57** 972
Spear K E and Dismukes J P 1994 *Synthetic Diamond: Emerging CVD Science and Technology* (New York: Wiley–Interscience)
Steeds J W, Charles S J, Davis T J and Griffin I 2000 *Diamond Relat. Mater.* **9** 397
Sternschulte H, Thonke K, Gerster J, Limmer W, Sauer R, Spitzer J and Munzinger P C 1995 *Diamond Relat. Mater.* **4** 1189
Sternschulte H, Horseling J, Albrecht T, Thonke K and Sauer R 1996 *Diamond Relat. Mater.* **5** 585
Sternschulte H, Thonke K, Sauer R and Koizumi S 1999 *Phys. Rev.* B **59** 12 924
Stiegler J, Bergmaier A, Michler J, von Kaenel Y, Dollinger G and Blank E 1998 *Diamond Relat. Mater.* **7** 193
Talbot-Ponsonby D F, Newton M E, Baker J M, Scarsbrook G A, Sussmann R S and Whitehead A J 1998 *Phys. Rev.* B **57** 2302 and references therein
Twitchen D J, Newton M E, Baker J M, Tucker O D, Anthony T R and Banholzer W F 1996 *Phys. Rev.* B **54** 6988
Twitchen D J, Newton M E, Baker J M, Tucker O D, Anthony T R and Banholzer W F 1999a *Phys. Rev.* B **59** 12 900
Twitchen D J, Hunt D C, Wade C, Newton M E, Baker J M, Anthony T R and Banholzer W F 1999b *Physica* B **273–4** 644
Twitchen D J, Baker J M, Newton M E and Jonston K 2000 *Phys. Rev.* B **61** 9
Twitchen D J, Newton M E, Baker J M, Anthony T R and Banholzer W F 2001 *J. Phys.: Condens. Matter* **13** 2045
van Oort E, Mason N B and Glasbeek M 1988 *J. Phys. C: Solid State Phys.* **21** 4385
van Oort E, Stroomer P and Glasbeek M 1990 *Phys. Rev.* B **42** 8605
van Wyk J A and Woods G S 1995 *J. Phys.: Condens. Matter* **7** 5901
van Wyk J A, Tucker O D, Newton M E, Baker J M, Woods G S and Spear P 1995 *Phys. Rev.* B **52** 12 657
Vermeulen L A and Halperin A 1981 *J. Phys. Chem. Solids* **42** 115
Walker J 1976 *Nature* **263** 275
Walker J 1979 *Rep. Prog. Phys.* **42** 1605
Watanabe K, Lawson S C, Isoya J, Kanda H and Sato Y 1997 *Diamond Relat. Mater.* **6** 99
Watkins G D 2001 *Phys. Status Solidi* a **186** 167
Webb S W and Jackson W E 1995 *J. Mater. Res.* **10** 1700
Weima J A, Zaitsev A M, Job R, Kosaca G, Blum F, Grabosch G, Fahner W R and Knopp J 2000 *J. Solid State Electrochem.* **4** 425
Werner M and Locher R 1998 *Rep. Prog. Phys.* **61** 1665
Wesra J, Sitters R and Glasbeek M 1992 *Phys. Rev.* B **45** 5699
Wight D R, Dean P J, Lightowlers E C and Mosby C D 1971 *J. Lumin.* **4** 169
Wilson J and Jubber M 1999 *Diamond Thin Films* (London: Taylor and Francis)
Yamamoto N, Spence J C H and Fathy D 1984 *Phil. Mag.* B **49** 609
Yelisseyev A P and Nadolinny V A 1995 *Diamond Relat. Mater.* **4** 177
Zaitsev A M 1993 *Mater. Sci. Eng.* B **11** 179
Zaitsev A M 1998 *Handbook of Industrial Diamonds and Diamond Films* ed M Prelas, G Popovici and L Bigelow (New York: Dekker) p 227
Zaitsev A M 2000 *Phys. Rev.* B **61** 12 909
Zaitsev A M 2001 *Optical Properties of Diamond: a Data Handbook* (Berlin: Springer)
Zeinert A, von Bardeleben H J and Bouzerar R 2000 *Diamond Relat. Mater.* **9** 728
Zeisel R, Nebel C E, Stutzmann M, Gheeraert E and Deneuville A 1999a *Phys. Rev.* B **60** 2476
Zeisel R, Nebel C E and Stutzmann M 1999b *Appl. Phys. Lett.* **74** 1875
Zeisel R, Nebel C E, Stutzmann M, Sternschulte H, Schreck M and Stritzker B 2000 *Phys. Status Solidi* a **181** 45
Zhou X, Watkins G D, McNamara Rutledge K M, Messmer R P and Chawla S 1996 *Phys. Rev.* B **54** 7881
Zvanut M E, Carlos W E, Freitas J A Jr, Jamison K D and Helmer R P 1994 *Appl. Phys. Lett.* **65** 2287